2020·广州
世界5G大会
WORLD 5G CONVENTION

WIRELESS TECHNOLOGY TRENDS TOWARDS 6G

WHITE PAPER V7.0 D
2020.11

Executive Summary

The fifth generation (5G) wireless network will be deployed globally from 2020，and more capabilities and features of 5G network are also under standardization discussions. Many countries and industry organizations have begun the discussions on the vision, requirements and technical characteristics of 6G communication networks. Therefore, further analysis of the development trend of 6G wireless air interface technology will provide benefit suggestions for the upcoming research of 6G technology.

This white paper focuses on the future trend of air interface technologies based on the new scenarios and new requirements for 6G. In the future, 6G communications will have more stringent requirements on various key performance indicators (KPIs) in diverse scenarios. In order to address the aforementioned challenges, it is necessary to significantly improve the spectral efficiency, time delay, energy efficiency, etc. To deal with the above problems, on the one hand, the future 6G wireless air interface will evolve towards higher frequency bands, which can make full use of the large bandwidth to increase communication capacity and bring the users with ultimate communication experience. On the other hand, for conventional lower frequency band communications, advanced coding, modulation, waveform and multiple access schemes are required. Especially, dedicated schemes for special scenarios such as high mobility are highly evoked. Meanwhile, new antenna architectures and signal processing technologies with extremely large scale antenna array, such as reflective intelligent surfaces, distributed MIMO, holographic radio, and multi-dimensional networking, are gaining increased attentions due to their ability of significantly improving the spectrum efficiency of the system.

Meanwhile, it has almost become a consensus that AI will play an important role in the future 6G networks. However, compared with the extensive application of AI in core network, network operation and management, and even radio resource control/management in radio access network, the application of AI in air interface design is a relatively new topic. Given that the current expert-knowledge-based air

interface design is approaching the performance limit, it is unclear how AI can unleash its unique potential to make more efficient use of the limited radio resources. This white paper will make a preliminary discussion on the above problems, including the discussion of wireless learning framework, as well as the introduction of specific use cases such as channel estimation, channel feedback, multiple access design, etc.

Finally, we summarize and look forward to the development trend of air interface technologies. We hope this whitepaper could embody a concentrated reflection of the viewpoints and insights of the researchers towards the developments trend of 6G wireless air interface and provide some inspirations for the following research in this field.

Table of Contents

1 Introduction

With the 5th Generation (5G) Mobile network rolling out in 2019, research towards the next generation mobile network has been started across the world. One of the symbolic features of 5G system is that three major scenarios are proposed, i.e., enhanced mobile broadband (eMBB), ultra-reliable and low latency communication (URLLC), and massive machine type connection (mMTC), based on which specially designs and optimization have been made on each scenario. One of the biggest concerns of the moment is how future mobile networks will be, and how to realize these attractive visions through evolutionary or revolutionary technologies [1].

Some appealing visions towards future human life with the aid of next generation networks have been launched very recently. In 2030 and beyond, with the fast progress of informatization and digitalization of the society, a brand-new world of digital twin will be built in which each physical entity has a virtual replica. The digital world establishes a bridge, allowing seamless transmission of information and intelligence, between human and human, human and things, and even things and things in the living entity. The digital world is the simulation and prediction of the living entity which accurately reflects and predicts the real state of the living entity. These simulation and prediction of living entity from digital world may also be utilized to early intervene the operation of a living entity or the physical world and prevent the risks and disasters in advance. It helps human to further liberate themselves, improve life quality, production efficiency and social governance, and realize the great vision.

Governments and industry organizations around the world are also actively exploring next-generation wireless networks. The Finnish government has taken the lead in launching a 6G Flagship program worldwide, and held the first and second 6G Wireless Summit in 2019 and last month respectively. China has kicked off the work on 6G in 2018. The Federal Communications Commission of the United States has opened up the terahertz spectrum for 6G research. South Korea plans to achieve 6G by 2028. Meanwhile companies such as Samsung and LG have opened their 6G

research centers last year. Japan has set up a government-civilian research society in January, and announced plans to kick off 6G research. ITU created FG-NET-2030 in 2018, started IMT. FUTURE TECHNOLOGY TRENDS research in February, and plans to start the research work on new vision in the half year of 2021. Many industry white papers and academic papers have addressed the different aspects of 6G mobile network. For example, the vision, new applications and requirements of 6G are discussed from different aspects in [1][4], the potential enabling technologies of 6G is highlighted in [4][5][6], and the artificial intelligence (AI)'s applications in physical layer communication and network architecture are discussed in [1][6].

This white paper aims to investigate the next generation wireless communication systems from the perspective of technological development. First, the vision and requirements for the next generation of wireless networks will be briefly described. Next, we introduce the new technology for the next generation communication system from the point of view of typical air interface module design. In addition, the current eye-catching artificial intelligence (AI) technology will also play a pivotal role in the future air interface, so we use a dedicated chapter to introduce the air interface scheme based on artificial intelligence. Finally, based on the new technology introduced in the white paper, we summarize the future development trend of wireless air interface, providing insights for the researchers in this field.

2 Scenario requirements and fundamental theory of 6G air interface

2.1 6G new scenario

Towards 2030 and beyond, new application scenarios will emerge in endlessly. In general, the scenarios fall into three categories: intelligent life, intelligent production, and intelligent society [2], as shown in Fig. 2.1.

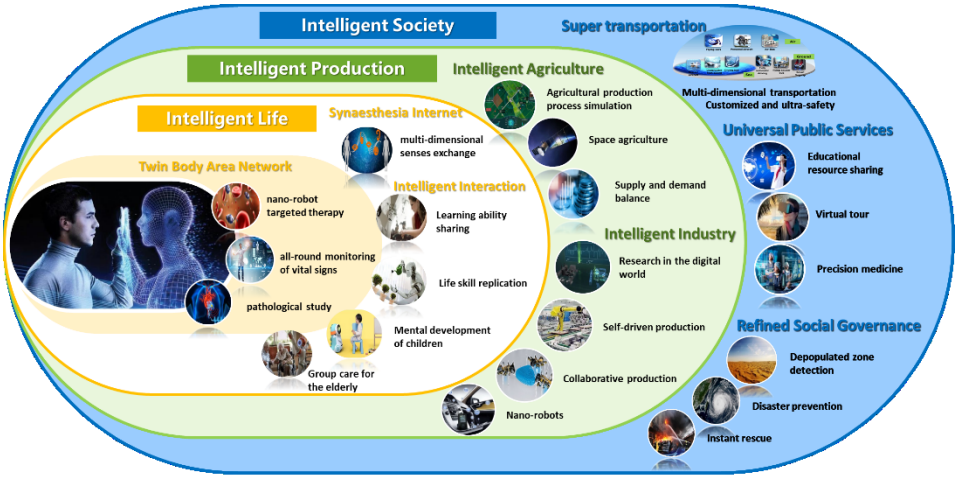

Fig. 2.1 Typical application scenario beyond 2030

(1) Intelligent Life: It is expected in 2030, synaesthesia internet, twin body area network, and intelligent interaction will reshape our life in the aspects of learning, shopping, working, and healthcare, etc.

(2) Intelligent Production: By applying emerging technologies to agriculture and industry, the healthy development of production could become true, leading to a rapid development of the digital economy. With 5G, the intelligent production will be initially realized through informatization methods. For example, human hands will be freed if intelligent devices such as drones are used in agricultural production. Manufacturing efficiency will be improved if devices such as robots and VR are used in manufacturing. With the more advanced technologies such as digital twins, it will certainly lead to a better intelligent production in 6G.

3) Intelligent Society: With the “ubiquitous coverage” network in 2030, the coverage of public service will be greatly expanded and thus the digital gaps between different regions will be narrowed. On the whole, 6G network will help to improve

the social governance and lay a solid foundation for building a better society.

2.2 6G requirements and the gap between 5G and 6G

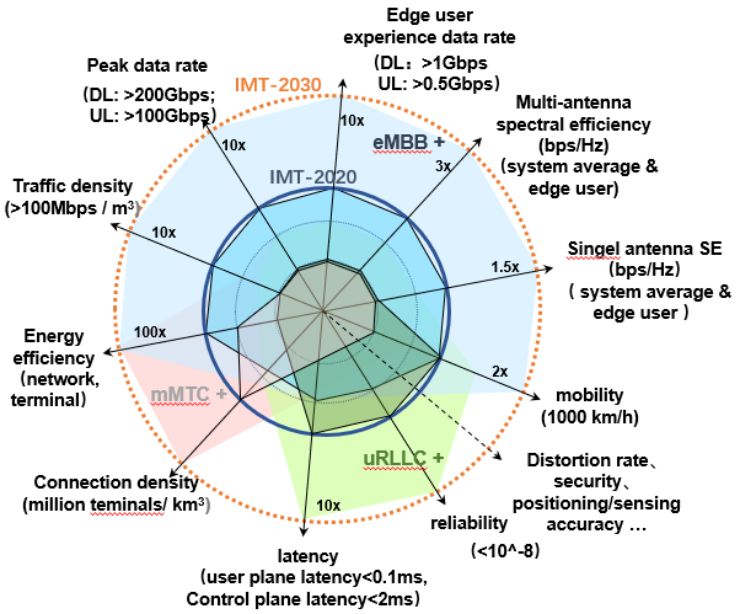

Fig. 2.2 KPI and requirements for 6G typical scenarios

Facing more diversified services and scenarios in the future, 6G scenarios include the further extension of the three current 5G scenarios: (1) eMBB+ for human-to-human communication scenarios. (2) URLLC+ for corresponding to autonomous things-to-autonomous things communication scenarios. (3) mMTC+ for corresponding to humans and autonomous things communication scenarios. Based on the analysis of 6G requirements and the performance of existing 5G standards, considering integrating future network business requirements and technical capabilities, the KPIs of 6G network capabilities are shown in Figure 2.2. The requirements are reflected in the improvement of existing 5G network KPIs, as well as some new KPIs.

Based on the comprehensive analysis of current 5G network capabilities, the forecast of future wireless communication traffic and the judgments of 6G potential technology enablers, 6G network KPIs are different from 5G in following aspects:

(1) 6G has more challenges in spectrum efficiency. Single-antenna (port) system average spectrum efficiency and edge spectrum efficiency (SE) may be considered. The purpose is to pave way for more high SE transmission technologies, rather than

relying solely on the increase in the number of antennas, bandwidth, base station density and other resource-consuming solutions.

(2) Energy efficiency (EE) are tightly bounded with SE at high network load region. EE at low network load region mainly depends on the sleep duration of base stations and terminals. Therefore, it is not accurate to evaluate system EE based on the sleep ratio alone. In addition, there is a big difference between the system's SE and EE for high load. If the SE of the system is improved, the required power consumption is also increased in the same proportion. In addition, the power consumption of equipment are various for different manufacturers. Therefore, from the perspective of standardization, it is recommended to specify the minimum system EE threshold requirements, promote the research of high energy-efficient air interface technology.

(3) The future 6G system may introduce 3D coverage scenarios, such as buildings, unmanned aerial vehicle (UAV), and ATG network. Therefore, 6G cells will become cubic, and the indicators such as traffic density and connection density in 5G are expected to expand to 3D density in 6G.

(4) In addition to improving single KPI such as spectrum efficiency, delay, and number of connections, 6G also needs to consider the joint optimization of multiple KPIs in future mixed scenarios. For example, in future high-speed train scenarios with extremely high requirements for mobility, user activation rate, data transmission rate, and coverage, the improvement of network SE will face unprecedented challenges. Therefore, the optimization of KPIs for hybrid scenarios needs to be considered comprehensively and treated differently. This also greatly increases the complexity of 6G demand indicator formulation.

(5) Cross-layer design for various traffics. 6G network KPIs may introduce traffic-related indicators to achieve end-to-end optimization design, such as distortion rate [1], positioning/perception accuracy [9], security [8], etc.

(6) More importantly, it is recommended that the scalability and flexibility of the network should be considered in the design of 6G network, and too much changes should be avoided during the network evolution to reduce the overhead of

standardization.

2.3 Fundamental theory

Wireless Security Theory: The two fundamental characteristics of the wireless medium, namely broadcast and superposition, present different challenges in ensuring reliable and/or secure communications in the presence of adversarial users. The broadcast nature of wireless communications makes it difficult to shield transmitted signals from unintended recipients, while superposition can lead to the overlapping of multiple signals at the receiver. As a consequence, detect and jamming are two main adversarial risks for wireless security issues.

While jamming and counter-jamming physical layer strategies have been of long-standing interest especially in military networks, such as frequency hopping and spread spectrum techniques, the security of data transmission has traditionally been entrusted to key-based enciphering (cryptographic) techniques at the network layer. In 6G, besides the conventional physical layer security, other types of security, such as integrated network security, should be jointly considered. Therefore, new security approaches, relying on low complexity and having high security levels, are attracting more intensive study, such as low-density parity check (LDPC)-based secure massive MIMO; secure mmWave techniques may also be suitable for UM-MIMO and THz band applications. Some advanced theories and techniques for wireless security are listed as follows.

Game theory: The interactions between various agents (transmitters, receivers, helpers, and attackers) in multiuser wireless networks are accurately captured by inter-disciplinary analyses based on game theory and microeconomics, and this holds true for problems of secrecy as well. Stable outcomes from which no player has an incentive to deviate are known as Nash Equilibria.

Blockchain-based Spectrum Management: Recently, blockchain has gained attention because it can provide a secure and distributed database for all transaction records (i.e., blocks) by enabling all participants to record blocks, each of which includes the previous block's cryptographic hash, a time stamp, and transaction data.

This model is suitable for the characteristics of spectrum sharing. Therefore, blockchain-based spectrum management is a promising technology for 6G to provide secure, smarter, low-cost, and highly efficient decentralized spectrum management.

Quantum Communications: Quantum communications can provide strong security by applying a quantum key based on the quantum no-cloning theorem and uncertainty principle. When eavesdroppers want to carry out observations or measurements or copy actions in quantum communications, the quantum state will be disturbed, and the eavesdropping behavior can be easily detected. Theoretically, quantum communications can achieve absolute security.

3 Advanced air interface technologies towards 6G

3.1 Coding and modulation

From 4G to 5G, the peak rate of uplink and downlink increases by 10-100 times, and this trend is likely to continue to 6G. It is predicted that the throughput of a single decoder may reach hundreds of Gbps. It is difficult to achieve such a high throughput goal only depends on the progress of IC manufacturing technology in 10 years. Solutions must be found from the algorithm aspect as well. Compared with polar code and turbo code, quasi-cyclic LDPC code has a very high degree of parallelism, and is very suitable for high-throughput services. New designed ultra-high speed LDPC codes are expected to meet the requirements of 6G data channel. Both new parity matrices design and corresponding encoding/decoding algorithms need to be taken into account to reduce the decoding iterations and improve decoder's parallelism level. It is also vital for a decoder to keep a reasonable power consumption level. Considering dramatically increased throughput requirement, the energy consumption per bit needs to be further reduced by at least 1~2 orders of magnitude.

Modulation is another technique that 6G can re-examine. High order QAM constellation modulation has been used to improve spectral efficiency. However, because of the non-linearity of transmission medium, the marginal benefits obtained in higher-order QAM constellations are gradually disappearing. New modulation methods, for example, schemes based on signal shaping, have been proved to be effective in wired communication or broadcast system. However, whether they are also applicable to wireless communication is worth careful study.

One of the promising solutions is probabilistic shaping (PS). By using the same QAM constellation by transmitting different constellation points at different probabilities, PS schemes can approximate the optimal Gaussian distribution for approaching the Shannon limit. Because of its low-complexity implementation, a PS scheme called probabilistic amplitude shaping (PAS) gains much attentions in these years. It is shown that PAS can achieve an FER around 0.01 within 1.1 dB to the AWGN capacity from 1 bits/dim to 5 bits/dim at a step of 0.1 bits/dim using the

DVB-S2 LDPC codes without iterations between demodulation and decoding. Recently, it is shown that PAS combined with NR-LDPC codes can have coding gains more than 2 dB compared to the current 5G modulation and coding schemes over AWGN channels at some settings. These results show that signal shaping is a direction worth consideration in developing 6G.

Reducing the peak-to-average-power-ratio (PAPR) is an important technology direction in order to enable IoT with low-cost devices, edge coverage in THz communications, industrial-IoT applications with high reliability, etc. Some low PAPR modulation schemes, such as FDSS+pi/2 BPSK, 8-BPSK and CPM, were proposed, but which had some loss in the demodulation performance when obtaining the lower PAPR. So more research is still need for low PAPR modulation schemes with good performance. The phase noise is very high in TeraHertz band. Although the receiver can compensate the most, the residual phase noise will still impact the performance. So new modulation scheme with good suppressing phase noise capability is another important technology direction in THz band. New demodulation algorithm also needs to be researched due to the different characteristic between phase noise and AWGN.

Furthermore, to meet the dramatically increased throughput requirement of 6G, there are only two solutions. One is to use wider spectrum, the other is to increase spectral efficiency. THz communication and visible light communication can provide wide spectrum, but are limited by coverage. Thus, it is urgent to increase spectral efficiency. Some high spectral efficiency modulation technologies, such as FTN(faster-than-Nyquist) and SEFDM(spectrally efficient frequency division multiplexing), has been proposed for several years, which are worthy of being studied further to investigate their performance.

3.2 Waveform and multiple access

There will be more scenarios for different services in 6G. Different scenarios have different requirements. Enhanced waveform design will be crucial in specific scenarios to guarantee the performance. No single waveform solution addresses the

requirements of all scenarios. For example, high frequency scenario is faced with some challenges, such as higher phase noise, larger propagation loss due to high atmospheric absorption and lower power amplifier efficiency. Waveform based on single carrier form may be a good selection for high frequency scenario to overcome these challenges. For indoor hotspot, the requirements include larger capacity, higher data rate and flexible user scheduling. Waveform based on CP-OFDM form may be a good selection for the scenario. For higher Doppler frequency shifts scenarios, the transformed domain waveform based on OTFS may be an effective approach to harvest the gain of Doppler domain diversity. So multiple waveform schemes will be designed to satisfy different requirements in 6G. Case-by-case system optimization will be needed and compatibility across different waveforms must also be redefined.

Multiple access technology has played an important role in wireless communication in the last decades. It can increase the capacity of the channel and allow different users to access the system simultaneously. Generally, multiple access can be classified as grant-based multiple access and grant-free multiple access. Grant-based multiple access requires dedicated multiple access protocols to coordinate the communication of the accessible users in the systems. Grant-based multiple access technology has become mature and been adopted by various wireless communication standards. However, the grant-based multiple access technology, designed for current human-centric wireless networks, is not appropriate for future autonomous thing-centric wireless networks. To support millions of devices in the future cellular network, a fundamental rethink of the conventional multiple access technologies is required in favor of grant-free schemes suited for massive random access. Grant-free multiple access does not need to perform a sufficient coordination among the users, and can more efficiently handle the low latency requirement, global scheduling information deficiency, or the bursty and random access pattern of user activity, etc. Grant-free multiple access technology has been used in the initial access process of both cellular terrestrial and satellite communication networks. There are also some challenges for grant-free multiple access, for example, the performance

limit for massive bursty devices simultaneously transmitting short packets; the low complexity and energy-efficient channel coding and communication schemes for massive access; efficient detection methods for a small number of active users with sporadic transmission.

3.2.1 Multi-carrier waveform

As the baseline of multi-carrier waveform, the main idea of CP-OFDM is to divide the channel into several orthogonal sub-channels, transform the high-speed data flow into the low-speed data flows, and then modulate to each orthogonal sub-carrier to transmit. In OFDM systems, cyclic prefixes are added at the transmitter to avoid inter-symbol interference and inter-subcarrier interference caused by multi-path. In addition to CP-OFDM, the new multi-carrier waveforms also include F-OFDM, UFMC, FBMC, and, etc.

3.2.1.1 Flexible OFDM

Several new multi-carrier modulation schemes have been proposed, e.g. universal filtered multi-carrier (UFMC), generalized frequency division multiplexing (GFDM) and filter bank multi-carrier (FBMC), and Filter-OFDM (F-OFDM). The flexible compatible framework for theses waveforms can be based on the carrier/waveform aggregation. Different waveforms located in different carriers can be aggregated in one air interface serving diverse 5G services. The waveform, sub-band bandwidth, subcarrier spacing bandwidth, filter length and cyclic prefix (CP) length in each wave can be flexibly chosen according to the dedicated scenarios and services [10].

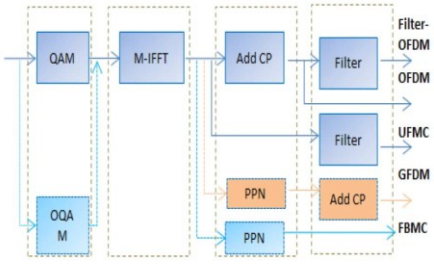

Fig. 3.1 A unified framework of flexible waveforms [10]

A common feature of these new waveforms is that filters are employed to suppress the out of band emission and relax the requirement on time-frequency synchronization. But there are also subtle differences among these waveforms. The filters in UFMC and F-OFDM are implemented at the granularity of each sub-band. The main difference is that F-OFDM uses a longer filter and the signal processing procedure is same as the conventional OFDM in each sub-band for backward compatibility. In contrast, UFMC uses a shorter filter and the CP of OFDM is replaced with empty guard period. GFDM can cover CP-OFDM as special cases according to different number of subcarrier and sub-symbol in a GFDM block. In addition, the overhead is kept small by adding CP for an entire block that contains multiple sub-symbols. The filter in FBMC is implemented at the granularity of each subcarrier. By a well-designed prototype filter, FBMC can well suppress side-lobes of a signal. Moreover, the overhead can also be reduced by removing CP in FBMC as UFMC. At the same time, in order to reduce the interference of adjacent sub-channels and computation complexity, the orthogonal Quadrature Amplitude Modulation (OQAM) modulation and poly-phase network (PPN) is needed in FBMC and GFDM schemes.

$$x(t)=\sum_{u\in U}\sum_{k\in K_u}\sum_{n=-\infty}^{+\infty}\sum_{m=1}^{M}s_{k,n}(m)\cdot g_{k,m}(t-nT)e^{j2\pi f_k(t-nT)}\otimes h_u(t)$$

According to the available research results, there does not exist a multi-carrier modulation scheme to support diversified requirements. In the following, we propose a compatible multi-carrier modulation structure with low complexity as depicted in Fig. 3.1, which can also be represented as the formula above, where $s_{k,n}(m)$ is the m-th subsymbol in the *n*-th transmission symbol and *k*-th subcarrier. $g_{k,m}(t)$ is the shaping filter in a single symbol. The filter of each user is denoted as $h_u(t)$. And the frequency of subcarrier is denoted as f_k. The symbol duration is *T*. And the convolution operator is denoted as $\otimes$.

3.2.1.2 Orthogonal time frequency space (OTFS)

Recently, a novel modulation system called Orthogonal time frequency space (OTFS) was proposed for the sake of exploiting full diversity over time and frequency resources in the delay-Doppler domain. In OTFS systems, the transmit symbols undergo a near-constant channel gain in the delay-Doppler domain, thus it is suited in future communication scenarios compared to traditional Orthogonal Frequency Division Multiplexing (OFDM) techniques.

To further improve the spectral efficiency, multiple-input multiple-output (MIMO) was suggested to combine with OTFS systems. In MIMO-OTFS, the system can not only get the time and frequency diversity due to the OTFS structure, but also get the space diversity due to the MIMO structure. Specifically, the transmit symbols go through from the Doppler-delay domain to the time-frequency domain in the transmitter, and the inverse process in the receiver. The above process can obtain full time and frequency diversity. On the other hand, in the MIMO setup, the symbols in each transmit antennas can reach to all the received antennas, this can obtain the space diversity.

Through the MIMO-OTFS can get the time, frequency and space diversity, it introduces high inter-symbol interference (ISI) and accurate inter-antenna synchronization (IAS) requirement. To alleviate the above effects, in the paper, we proposed a generalized spatial modulation OTFS (GSM-OTFS) system. Specifically, the GSM is a novel MIMO transmission technique that only employs a few radio frequency (RF) chains. Moreover, GSM can alleviate the ISI since it only activates parts of the antennas in each time slot. Thus we exploit the GSM structure to the OTFS system to obtain better system performance.

On the other hand, the decision feedback equalizer based on the minimum mean square error (MMSE) criterion is proposed for the new GSM-OTFS systems to get better system performance. The basic principle of the decision feedback equalizers is as follows. Specifically, the decision feedback equalizer includes two filters: the feedforward frequency domain equalization (FDE) filter and the feedback time

domain equalization (TDE) filter. The feedforward FDE filter is first employed to the receiver, thus the initial estimation symbols are obtained in the frequency domain (FD). Then the initial estimation symbols are transformed from the FD to the time domain (TD). Finally, the feedback TDE filter is employed to eliminate the ISI among the transmit antennas. Moreover, the parameters derivation of the feedforward FDE filter and feedback TDE filter are based on the MMSE criterion.

In this section, a full comparison in terms of bit error rate (BER) performance under the assumption of ideal channel state information in the receiver is given. The Extended Vehicular A (EVA) channel model is employed. Otherwise, M = 256 sub-carriers and N = 6 frames are assumed in the simulation. The BERs of the proposed GSM-OTFS, GSM-OFDM, MIMO-OTFS systems with Nt = 4 transmit antennas, Nr = 4 receive antennas are compared. On the other hand, in the proposed GSM-OTFS system, the proposed DFE can achieve better performance than the linear MMSE FDE. Specifically, the proposed DFE can converge in 3 times, and it can attain around 3 dB SNR gain at the BER of 10^{-4} compared to the linear MMSE FDE. In Fig. 3.2, the similar trend can be obtained. The system parameters of the Fig. 3.2 are Nt = 8 transmit antennas, Nr = 8 receive antennas in these three systems. Otherwise, the activated transmit antenna Na = 2 and QPSK modulation mode are assumed in the GSM-OTFS and GSM-OFDM systems, while BPSK modulation mode is employed in the MIMO-OTFS system.

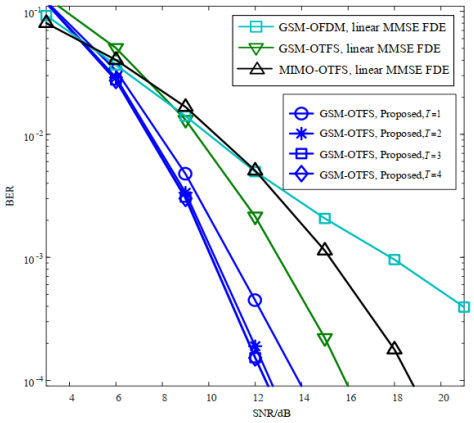

Fig. 3.2 Performance comparison among various systems and detectors with Nt = 8, Nr = 8, M = 256, N = 6.

3.2.1.3 Non-Orthogonal Waveform (NOW)

High frequency bands with large bandwidth (e.g., millimeter-wave and terahertz frequencies) are promising for 6G, but the system design is restricted by the non-linearity of power amplifier (PA). Multi-carrier waveform of CP-OFDM may not be suitable for high frequency bands due to its high peak to average power ratio (PAPR). Single carrier waveform represented by DFT-s-OFDM with low PAPR is promising. Considering the extreme high data rate requirement of 6G, how to keep the low PAPR of DFT-s-OFDM and improve its spectral efficiency (SE) will be the challenge especially when high-order modulation is not applicable.

1. Transceiver design of NOW

A non-orthogonal waveform (NOW) is proposed to improve the SE of DFT-s-OFDM [11]. The transceiver structure of NOW is shown in Fig. 3.3. There are three important modules to be designed, namely subcarrier mapping, FTN modulation and FTN demodulation.

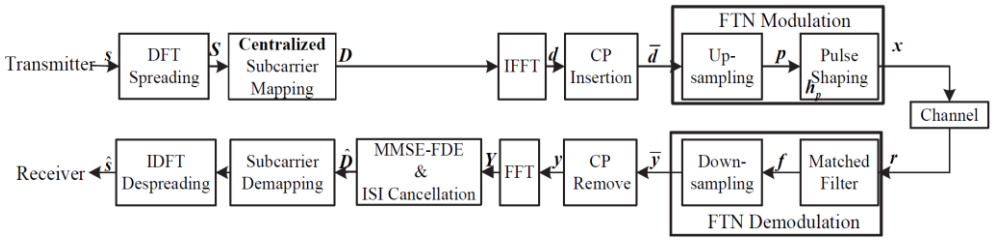

Fig. 3.3 The transceiver structure of proposed NOW scheme

(1) Centralized Subcarrier Mapping

Symbols after N-point DFT are mapped to N subcarriers for system bandwidth with N_1 subcarriers. For the proposed NOW transmitter, the symbols will be mapped into localized subcarriers in low frequency, which is called as centralized mapping method. It can be regarded as a special case of localized mapping method.

After centralized subcarrier mapping, the symbols are input into the IFFT module, parallel-to-serial conversion and CP insertion successively.

(2) FTN Modulation

FTN modulation is performed to the signals after CP insertion. The continuous-time FTN symbol can be written as $x(t) = \sum_{m=0}^{M+2v-1} \bar{d}(m)h(t - m\alpha T)$,

where $\bar{d}(m)$ denotes the m-th symbol of $\bar{\boldsymbol{d}}$ as shown in Fig. 3.3, M and $2v$ are the IFFT size and CP length, respectively, $h(t)$ is a T-orthogonal baseband transmission pulse, and α is the time domain compression factor ($0 < \alpha \leq 1$). The data symbols are transmitted $1/\alpha$ times faster than Nyquist signal, hence the transmission symbol rate is $1/\alpha T$.

Considering the discrete-time model signaling, the FTN modulation contains two discrete-time signal processing modules, up-sampling and pulse shaping, as illustrated in Fig. 3.3. (a) Up-sampling inserts zero-valued samples between adjacent data symbols, and the number of zero-valued samples for NOW is determined by α. (b) Pulse shaping filter is sampled at up-sampling rate and then performed linear convolution with the up-sampled signal.

(3) FTN Demodulation

At the receiver side, FTN demodulation is added for NOW, which also contains two discrete-time signal processing modules, matched filter and down-sampling. (a) Matched filter has the same pulse shape used at the transmitter side and sampled from $h^*(t)$ by the Nyquist up-sampling interval. (b) Down-sampling extracts useful samples from the received signal.

The MMSE-FDE after FFT module as described in [12] is used to eliminating the interference resulting from the FTN.

2. Impact analysis of time domain compression factor α for NOW

As one of the most important parameters for NOW, the time domain compression factor α can affect various performances. Link-level evaluation results of BLock-Error-Rate (BLER), throughput and SNR performance, and PAPR performance are provided below.

As shown in Fig. 3.4, when the time domain compression factor is smaller than one threshold (0.95 in the figure), no BLER reduction is observed. With the decrease of time domain compression factor, BLER becomes worse. This is because the useful signal spectrum will be truncated by the pulse shaping filter, which will result in partial information loss and increase the transmission error rate as analyzed in [1].

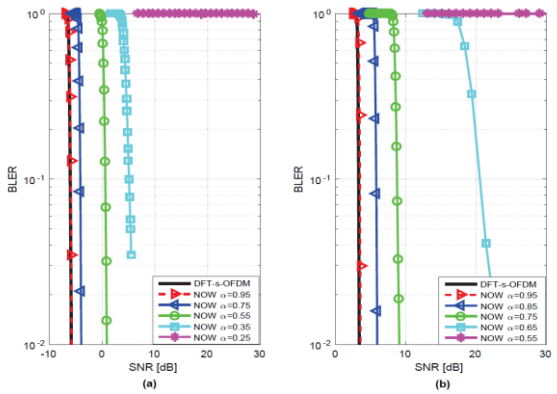

Fig. 3.4 BLER for DFT-s-OFDM and NOW with different α: (a) QPSK, (b) 16QAM.

$\alpha_{\text{opt}} = 0.95$ for NOW.

The smaller α is, the larger throughput gain can be achieved. But according to the analysis of the Power-Spectrum-Density (PSD) of the transmitting signal, α smaller than one threshold will result in signal truncation and hence SNR loss. Link-level evaluation results in Table 3.1 show throughput gain under different compression factors of NOW compared with orthogonal waveforms DFT-s-OFDM and CP-OFDM under QPSK and 16QAM. It is shown that compared with orthogonal waveforms, throughput gain can be achieved by NOW at the expense of SNR loss.

Table 3.1 Throughput gain and SNR loss of NOW

Compression factor	QPSK		16QAM	
	Throughput gain	SNR loss (dB)	Throughput gain	SNR loss (dB)
0.95	2.2%	0	2.2%	0
0.85	12.6%	1.2	12.6%	2.5
0.75	25.5%	1.9	25.5%	7.0
0.65	41.1%	3.0	41.1%	16.0
0.55	60.7%	4.3	–	–
0.45	86.0%	6.0	–	–
0.35	108%	10.0	–	–

PAPR performance of NOW is also evaluated. Results in Fig. 3.5 show that the PAPR of NOW is not only determined by modulation order and the number of subcarriers, but also determined by the time domain compression factor α. It is also shown that when other influencing factors are given, the PAPR firstly decreases and then increases with α, i.e., there will be an optimal α to achieve the minimal PAPR.

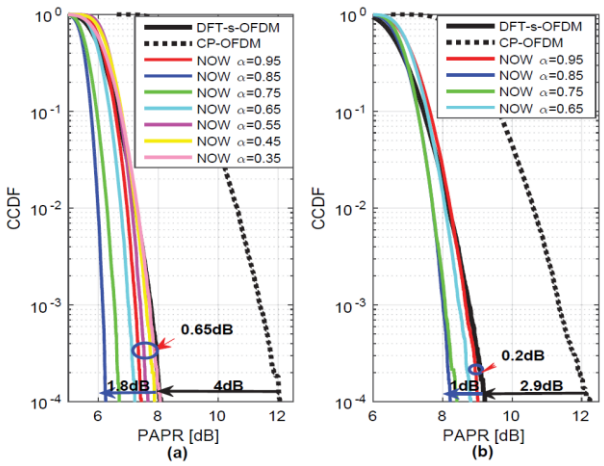

Fig. 3.5 PAPR of CP-OFDM, DFT-s-OFDM and NOW with different α: (a) QPSK, (b) 16QAM.

Therefore, the proposed NOW scheme can achieve both throughput gain and PAPR gain over the traditional orthogonal waveforms DFT-s-OFDM and CP-OFDM, by flexibly adjusting the compression factor.

3.2.2 Single carrier waveform

3.2.2.1 SC-FDE

SC-FDE is a single-carrier waveform based on frequency domain equalization. The processing at the transmitter and receiver is shown in Fig. 3.6.

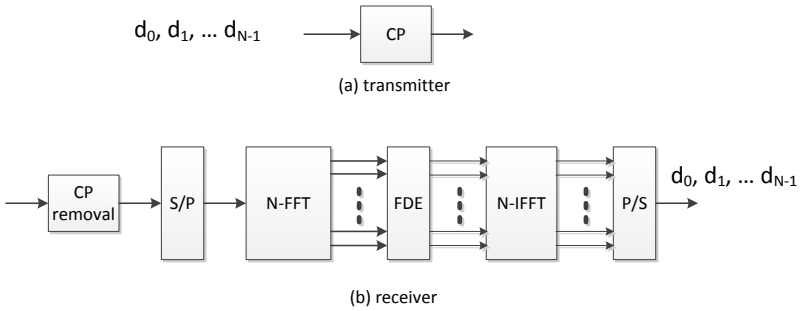

Fig. 3.6 The Tx-Rx link flow of SC-FDE

At the receiver, the received signal is transformed to the frequency domain through FFT with N points, and after equalization in the frequency domain, it is transformed to the time domain through IFFT with N points and output after serial-to-parallel conversion.

3.2.2.2 DFT-s-OFDM

The DFT spread based OFDM is called DFT-s-OFDM, and has following characteristics:

- The instantaneous power of transmit signal is changed slightly;
- The low complexity and high quality equalization can be used in the frequency domain;
- The allocation of bandwidth is flexible.

(1) The sub-classes of DFT-s-OFDM

The general process of standard DFT-s-OFDM processing is shown in Fig. 3.7, that is, the DFT transformation of M modulated symbols is first performed, and the output is mapped to the sub-carrier which is used as the input of IFFT with N points.

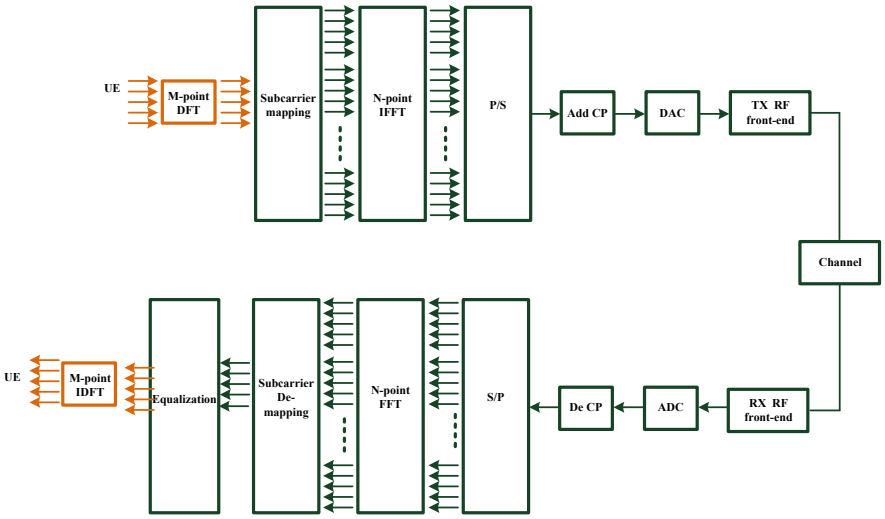

Fig. 3.7 The progress of DFT-s-OFDM

ZHT-FT-s-OFDM is based on the deformation of DFT-s-OFDM. ZHT-DFT-s-OFDM waveform is characterized by replacing the traditional CP filling by zero filling to the input of DFT with M points, with less CP overhead.

The size of input of DFT with M points can be changed based on the variation of channel delay expansion. The out-of-band leakage can be restrained by the method of the zero filling, thus saving CP overhead.

The implementation process of ZHT-DFT-s-OFDM is shown in Fig. 3.8.

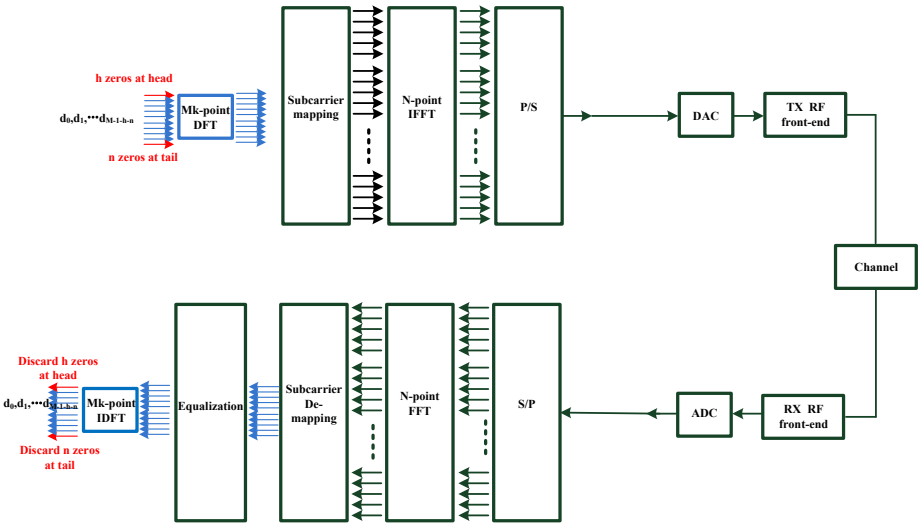

Fig. 3.8 The process of ZHT-DFT-s-OFDM

The GI-DFT-s-OFDM waveform is generated based on the deformation of ZHT-DFT-s-OFDM. Zeros are filled at the end of the input of the DFT with M points, and at the same time, the protection space x_{GI} is added to the output of IFFT, as shown in Fig. 3.9.

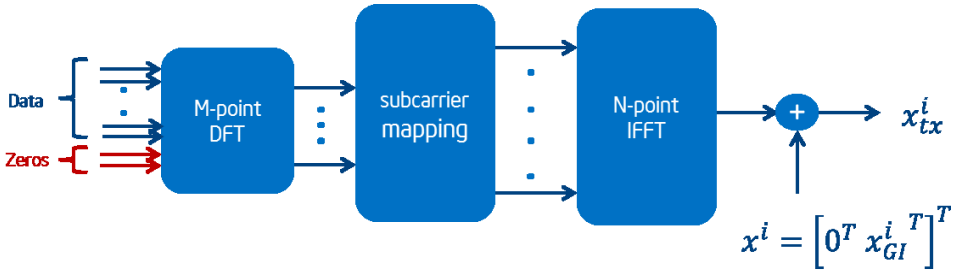

Fig. 3.9 The transmitter of GI-DFT-s-OFDM

And the receiver is shown in Fig. 3.10.

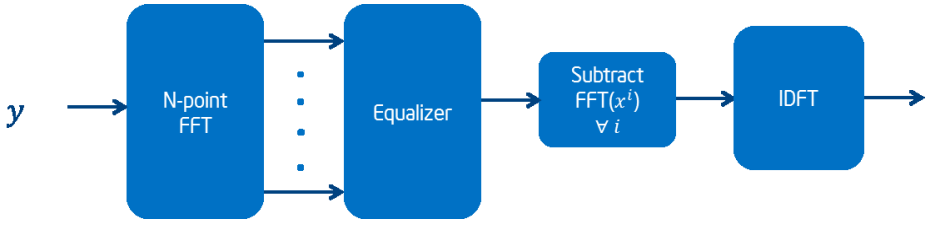

Fig. 3.10 The receiver of GI-DFT-s-OFDM

Where, the selection of GI sequence needs to meet the following characteristics:

- Good autocorrelation, that is, for any original sequence and the sequence generated by its cyclic shift are not correlated, the autocorrelation peak is sharp.

- Good cross-correlation, i.e. cross-correlation and partial correlation values close to 0.

UW-DFT-s-OFDM waveform is another deformation based on DFT-s-OFDM. A specific sequence is added to the input of DFT with M points at the beginning and end. If the specific sequence is a 0 sequence, that is, the UW-FT-S-OFDM is regressed to ZHT-FT-S-OFDM. The UW sequence can be defined in advance to perform other functions at the receiver, such as synchronization in time-frequency domain, channel estimation, frequency offset estimation, and so on. The process of UW-DFT-s-OFDM is shown in Fig. 3.11

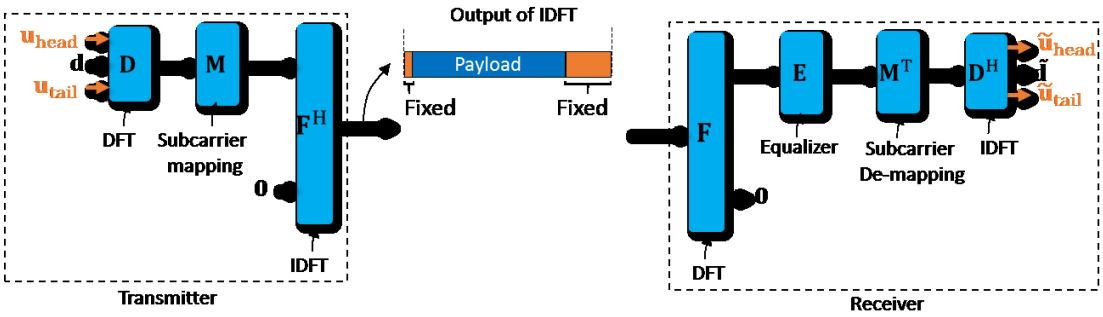

Fig. 3.11 The process of UW-DFT-s-OFDM

Although UW-DFT-s-OFDM does not use CP to avoid interference between symbols, the end of the previous symbol and the beginning of the current symbol can be roughly regarded as the same sequence.

(2) Resource mapping

The resource mapping methods of DFT-s-OFDM can be divided into two types: centralized and distributed. Centralized means that different users map the output of DFT with M points to continuous subcarriers, while distributed means that different users map the output of DFT with M points to the entire carrier range, and different users exist in an interleaving form.

Fig. 3.12 is a schematic diagram of centralized resource mapping of DFT-s-OFDM, and the DFT size can be different for different UEs, that is, bandwidth can be flexibly allocated to different UEs.

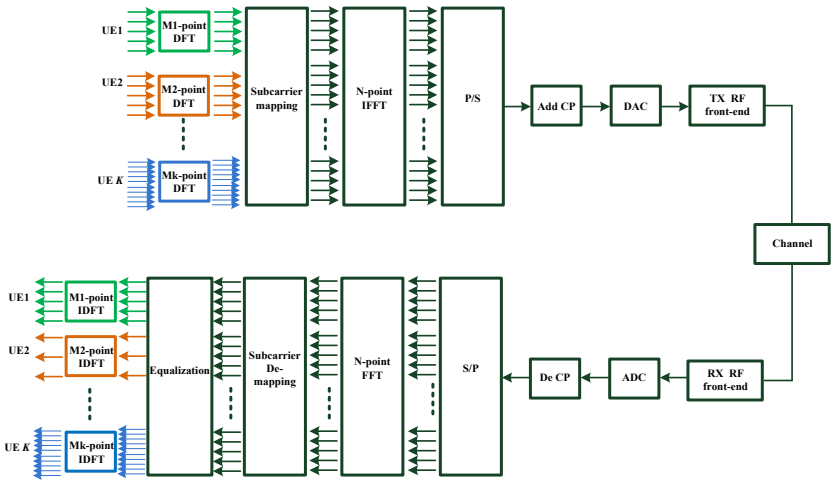

Fig. 3.12 Centralized resource mapping

Distributed resource mapping can also realize the reuse of users in frequency domain and flexible bandwidth allocation, but in this case, different users will exist in the frequency domain in an interleaving form. Compared with the centralized mapping, the distributed mapping is more sensitive to frequency error and has higher requirements on power control. Fig. 3.13 is a schematic diagram of the distributed resource mapping of DFT-s-OFDM.

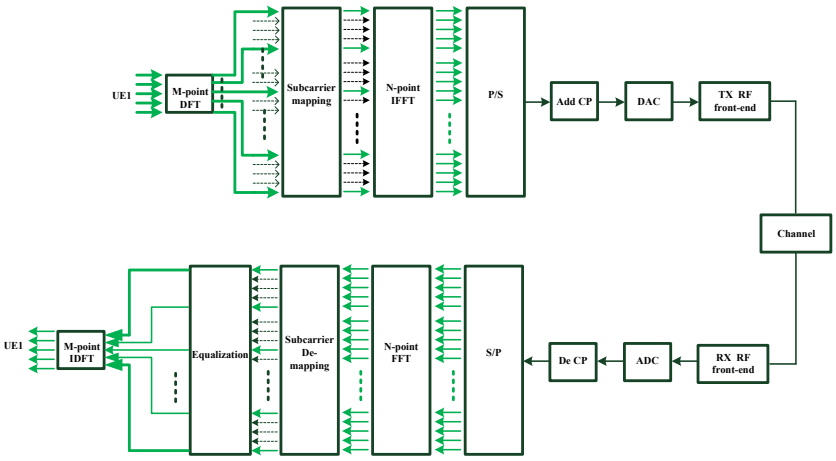

Fig. 3.13 Distributed resource mapping

(3) Performance

Fig. 3.14 shows the performances of PAPR corresponding to different DFT-s-OFDM waveforms with QPSK and 16QAM modulation.

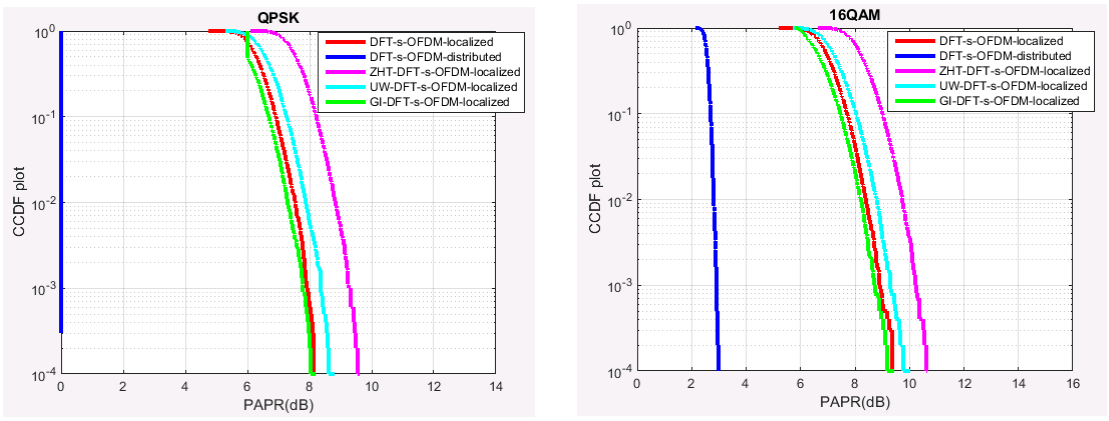

Fig. 3.14 The performance of PAPR

It can be seen that the PAPR of the distributed DFT-s-OFDM is the smallest, and the PAPR of the ZHT-DFT-s-OFDM is largest. The reason is that the zero filling of DFT with M points makes the average power of the sampling points after IFFT smaller, so the PAPR of the distributed DFT-s-OFDM waveform will be larger than other waveforms.

Fig. 3.15 shows the performances of CM (Cubic Metric) corresponding to different DFT-s-OFDM waveforms with QPSK and 16QAM modulation.

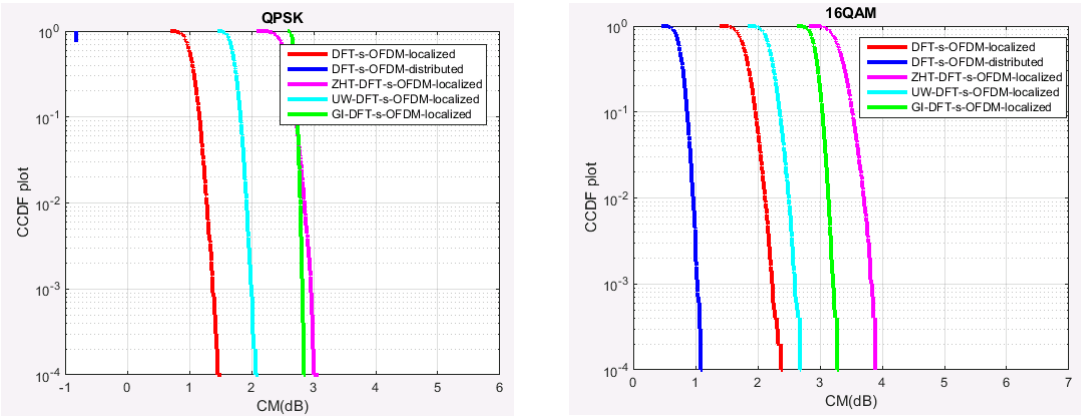

Fig. 3.15 The performance of CM

It can be seen that the CM of traditional DFT-s-OFDM is smaller than single carrier waveform.

3.2.2.3 SRRC

SRRC refers to Square Root Raised Cosine Filter, which is used in DVB (digital video broadcasting) system for baseband forming. The roll-off factor α of SRRC can be 0.35, 0.25 or 0.2 in DVB-S2/S2X and is fixed to 0.35 in DVB-S. The spectrum

efficiency is higher with a smaller α due to the steeper of the waveform.

The function of SRRC is

$$H(f)=\begin{cases}1 & 0\le|f|\le\dfrac{1-\alpha}{2T}\\ \sqrt{\dfrac{1+\cos\left[\dfrac{\pi(2T|f|-1+\alpha)}{2\alpha}\right]}{2}} & \dfrac{1-\alpha}{2T}<|f|<\dfrac{1+\alpha}{2T}\\ 0 & |f|\ge\dfrac{1+\alpha}{2T}\end{cases}$$

We can get the in-phase component I and the orthogonal component Q after the baseband shaping, and multiply by $\sin(2\pi f_0 t)$ and $\cos(2\pi f_0 t)$, respectively, thus we can get the orthogonal modulation signal by adding these two products together.

3.3 Extreme-MIMO

In the last ten years, massive MIMO has made remarkable achievements in theoretical research and system design. It has been specified in 5G NR system, and has been commercially deployed in several countries. In order to meet the ultra-high requirements in spectrum efficiency and peak rate, extreme MIMO is one of the most important key technologies in 6G and beyond systems. Extreme-MIMO is more than the evolution of massive MIMO. In addition to having extreme large scale antennas, extreme-MIMO also involves new antenna array implementations, new deployments and new applications.

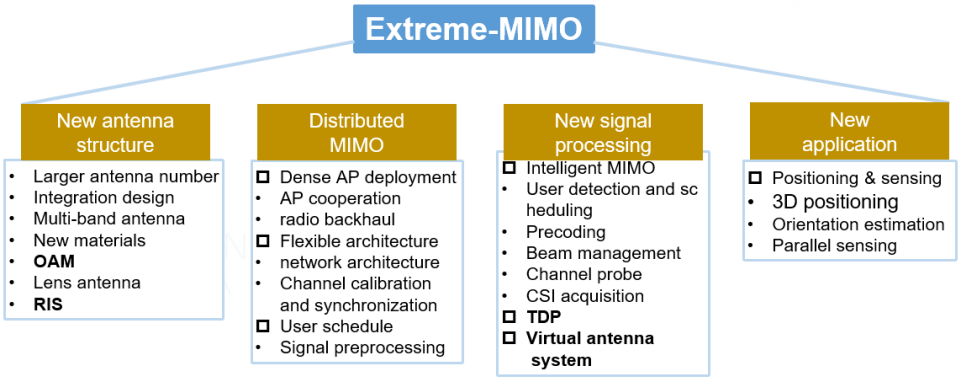

Fig. 3.16 The trend of extreme MIMO

As shown in Fig. 3.16, the trend of extreme-MIMO includes new antenna structure, distributed MIMO, new signal processing and new application. The

realization of extreme-MIMO depends on the development of antenna technology. From the perspective of performance, the number of antennas in extreme-MIMO system is expected to be much larger than massive MIMO. From the perspective of cost and network deployment, the array size, the array weight and the power consumption of the array are expected to be small. The development of extremely large scale antenna array follows the trend towards larger array scale, smaller array size, higher integration, higher frequency band and higher capability on multi-band transmission. The key technologies of extremely large scale antenna array include: new antenna structures and new antenna modes. The new antenna structures involve antenna designs of larger scale array in limited space, integration design of active antenna, antenna design based on new materials, multi-band antenna design, etc. The new antenna modes include lens antenna, RIS and OAM, etc.

Distributed extreme-MIMO deployment is an important trend of extreme MIMO. Compared to the centralized extreme-MIMO, distributed extreme MIMO system can provide higher spatial resolution and better performance. In addition, since the UEs and the access points are closer in the distributed extreme-MIMO system, the energy consumption of UEs can be significantly reduced. The development trend of distributed extreme MIMO system includes: ultra dense distributed access points deployment, flexible network architecture, user-centric scheduling. Compared to 5G distributed MIMO, the joint transmission capability among the access points of the distributed extreme MIMO would be significantly enhanced, and user-centric cell-free network architecture may be deployed. Through distributed extreme MIMO, undifferentiated users experience across the entire network is possible. The key technologies of distributed extreme-MIMO system include: network architecture design, access point cooperation technology, radio backhaul, synchronization and calibration, channel modeling, channel state information acquisition, signal preprocessing and signal processing technologies, etc.

Intelligence is another important trend of extreme-MIMO. The implementation of extreme-MIMO system requires a lot of decision-making and a lot of beam scanning.

The traditional algorithm may not guarantee the efficiency of extreme-MIMO. For example, pilots are used to estimate channel in current communication systems. The overhead of pilots increases linearly with the increase of the number of multiplexing streams and users. Then the efficiency of the system is reduced since less resources are allowed for data. Through AI technology, the relevant information of time, frequency, space and other dimensions can be used effectively, which may improve the performance of signal detection and reduce the cost of pilots. In the future, in order to make MIMO more efficiently and more intelligent, AI may be applied in the following modules of extreme MIMO system: channel probing, beam management, precoding, user detection and MU-MIMO scheduling, signal processing and CSI acquisition, access point allocation for distributed extreme-MIMO systems, etc. The intellectualization of extreme MIMO is not only reflected in the algorithm of the above modules, but also may involve the intelligent extreme-MIMO system architecture.

The application of high-precision beamforming for extreme-MIMO includes the application of extreme-high frequency band, three-dimensional coverage, high-dimensional positioning, sensing technology and so on. Although the extreme-high frequency band can provide extremely large bandwidth, the pathloss of signal is significant and the transmission is sensitive to atmospheric loss. By using extreme-MIMO to form a narrow beam with high beamforming gain, the coverage of extreme-high frequency band can be significantly improved. Hence, extreme MIMO would be a key technology to ensure the communication performance in extreme-high frequency band. Since the vertical beamforming granularity is coarse, vertical dimension can’t be well covered by massive MIMO. By forming high-precision vertical beamforming and applying distributed MIMO deployment, extreme MIMO can realize high-precision three-dimensional coverage. The high-dimensional positioning of extreme-MIMO evolves high-precision 3-dimensional geographical positioning and UE orientation estimation (i.e. roll, pitch and jaw). Estimation of the orientation in addition to geographical positioning has benefits for several

applications, such as automated vehicles, robots, VR, XR, etc. In additional to the geographical positioning, extreme MIMO can also achieve UE orientation estimation (i.e. roll, pitch and jaw). In the aspect of sensing, with the high spatial freedom, high spatial diversity gain and high spatial multiplexing gain provided by extreme-MIMO, the performance of target sensing can be significantly improved, the number of targets that can be sensed parallelly can be increased, and the interference suppression ability of sensing can be improved.

Although the extreme MIMO has lots of advanced characteristics compared with the massive MIMO, it faces many challenges. The main challenges of extreme MIMO system are: high cost, difficulty in channel modeling, high complexity of signal processing, large amount of computation, large delay of beam management, high pilot overhead, high pressure of fronthaul and backhaul transmission, high power consumption, etc.

3.3.1 New antenna structure

Reconfigurable intelligent surface (RIS), through a large number of low-cost reflective materials, makes the wireless transmission environment controllable and programmable, so as to improve the energy and spectrum efficiency of wireless networks. RIS can be regarded as a passive multi antenna technology deployed in the channel. Compared with the traditional active beamforming, the passive beamforming method of RIS creates a large number of phase shifted reflected signals to form wave interference, which affects the electromagnetic environment. In this way, a large number of RF links required in original active beamforming are simplified, and the cost is significantly reduced.

RIS includes large-scale device arrays and array control modules, as shown in Fig. 3.17. The large-scale device array is composed of a large number of device units regularly and repeatedly arranged on a flat bottom plate. Each device unit has a variable device structure. For example, the device unit contains a PIN diode, and the switching state of the PIN diode determines the response mode of the device unit to external wireless signals. The array control module of RIS can control the working

state of each device unit, thereby dynamically or semi-statically controlling the response mode of each device unit to wireless signals. The wireless response signals of each device unit of the large-scale device array are superimposed on each other to form a specific beam propagation characteristic on a macroscopic scale. The control module is the "brain" of the RIS. It determines the wireless signal response beam of the RIS according to the needs of the communication system, making the original static communication environment " intelligent" and "controllable".

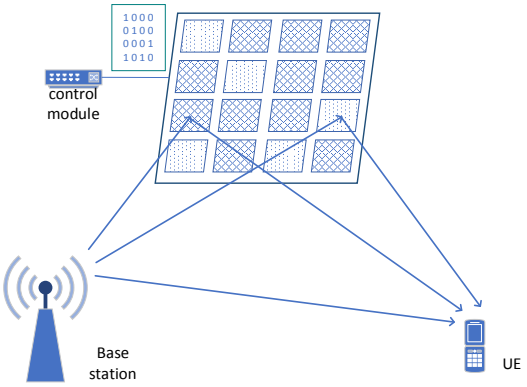

Fig. 3.17 Schematic diagram of RIS

RIS has been applied in many technical fields, and there are many different design schemes in different application scenarios. According to the physical principles of the device unit [13], the classification includes Tunable Resonator variable capacitance type, Guided Wave waveguide type, Element Rotation polarization type. According to the wireless signal output form, it is divided into reflective RIS and transmissive RIS. According to the wireless signal response parameter [14], the classification includes phase control RIS, amplitude control RIS and amplitude and phase joint control RIS. According to the response parameter control classification, it is divided into continuous control type and discrete control type. According to the frequency or speed of controlling the amplitude and phase of the RIS, it can be divided into static, semi-static/dynamically controlled RIS. Among them, static RIS can currently be applied to existing systems, such as 4G/5G systems. Considering the complexity of device design and fabrication, academia generally chooses discrete control device units with a single wireless signal response parameter for research. At present, the Intelligent Reflecting Surface (IRS), which is widely discussed in

academia, is a phase-controlled RIS based on signal reflection. The phase of the reflected signal of the device unit is controlled through 1 bit of indication information to achieve 0 or π phase reversal. Benefiting from the lack of radio frequency and baseband processing circuits, RIS devices have several advantages over traditional wireless communication transceivers:

(1) RIS has lower cost and implementation complexity;

(2) RIS has lower power consumption;

(3) The RIS will not introduce additional thermal noise at the receiving end;

(4) RIS devices are thin and light, and can be deployed flexibly.

The application scenarios of RIS are mainly divided into two categories: the low-cost multi antenna transmission scenario deployed near the transmitter, including passive beamforming, joint precoding and ultra-massive MIMO, and the energy coverage scenario deployed near the receiver, including NLOS coverage, edge user enhancement, and high-precision positioning. Future 6G communication services require higher communication rates and greater connection density [15], and need to utilize more spectrum resources and achieve higher spectrum efficiency. Many emerging technologies are considered to be potential technical directions of 6G communication systems, such as terahertz communication and ultra-large-scale MIMO technology. The combination of RIS technology and the above-mentioned technologies can improve the performance of communication systems in multiple practical application scenarios.

Obstructions in the wireless communication environment will cause shadow fading, resulting in signal quality degradation. Traditional wireless communication system improves the signal quality of the received signal by controlling the transmitting signal beam of the transmitting device and the receiving signal beam of the receiving device. For millimeter wave and terahertz frequency bands, the transmission and diffraction capabilities of high-frequency signals are weak, and the communication quality is more obviously affected by obstructions. The RIS can provide forwarded signal beams for blocked terminals to extend the coverage of the

cell, as shown in Fig. 3.18(a). For ultra-high-traffic hotspot services, such as VR services, the direct link between the base station and the terminal may not provide sufficient throughput. The RIS can provide additional signal propagation paths for hotspot users and improve the throughput of hotspot users, as shown in Fig. 3.18(b). RIS technology can be combined with massive MIMO technology to overcome the increase in cost and power consumption caused by the increase in the number of transmitting and receiving antennas, and improve the spatial diversity gain of MIMO while reducing equipment costs, as shown in Fig. 3.18(c). The 4G era introduced the concept of Massive MIMO and achieved significant performance gains. However, as the number of antennas increases, base stations require more RF links, resulting in higher power consumption and complexity, which greatly increases the cost of base stations and limits the further increase in the scale of Massive MIMO. RIS is an evolution technology direction of Massive MIMO. Since the RIS only reflects or refracts the incident signal, there is no need for a radio frequency link, which reduces hardware complexity and power consumption, and can further increase the scale of antenna array and obtain higher beamforming gain.

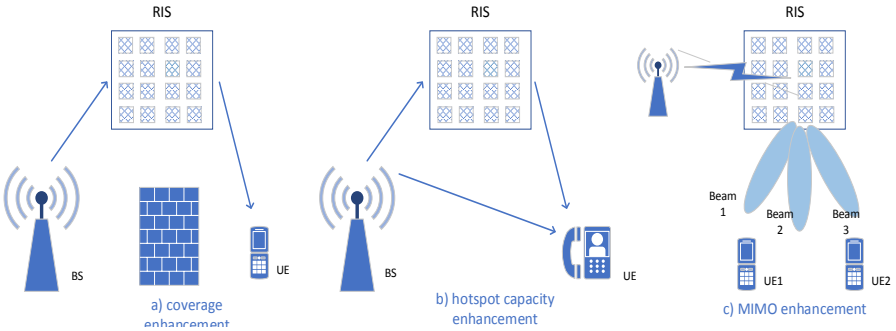

Fig. 3.18 Application scenarios of RIS

The communication system based on RIS has been tested in universities and research institutions, as shown in Fig. 3.19. In foreign countries, Japan's DOCOMO first tested 28 GHz millimeter wave communication based on static intelligent reflective surface in the field in 2019 [16], and the communication rate reached 560 Mb/s. In the same environment, the end-to-end communication rate without relying on smart reflective surface is only 60 Mb/s. The Massachusetts Institute of Technology in the United States has built a test platform RFocus [17] that works in

the 2.4 GHz unlicensed frequency band, which verified the feasibility of deploying RIS in indoor shopping malls. The indoor signal coverage after the deployment of RIS has been increased by about 2 times on average.

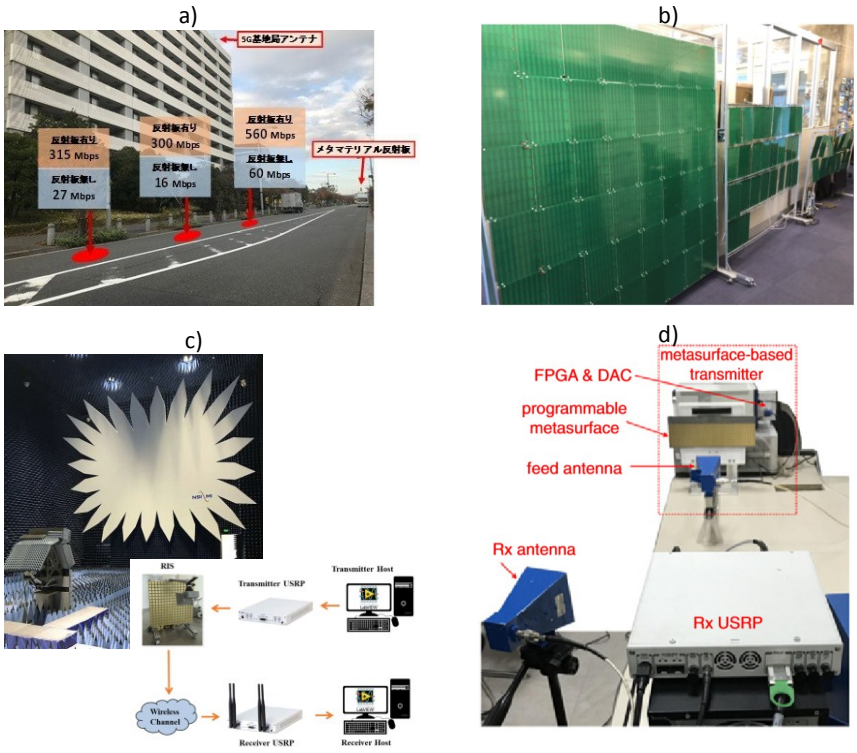

Fig. 3.19 Test platform of domestic and foreign research institutions

(1) NTT DOCOMO's outdoor environment millimeter wave test platform

(2) MIT's indoor RFocus test platform

(3) Tsinghua University beamforming test platform based on intelligent reflective surface

(4) Southeast University's 8PSK signal modulation test platform based on intelligent reflective surface

Domestic colleges and universities have also implemented communication systems based on RIS, and have unique insights in the structural design and system architecture design of RIS device units. Tsinghua University [18] designed a 2 bit discrete phase control device, which contains two PIN diodes as a 2 bit control module. Tsinghua University has produced an intelligent reflective surface with 256 device units. The beamforming gain of this device in the 28.5 GHz frequency band can reach 19.1 dB. Southeast University [19] designed a voltage-controlled intelligent

reflection device, which has a good voltage-reflection phase linear relationship. Based on this new device unit, Southeast University realized the 8PSK signal adjustment based on the intelligent reflective surface, and the communication rate reached 6.144 Mb/s. It is worth noting that, unlike traditional RIS that passively reflect or refract third-party signals, the RIS designed by Southeast University can also transmit the signals of the RIS itself by changing the phase of the third-party signals, which essentially can be seen as a backscatter technology.

The communication system based on RIS technology verifies the feasibility of this new technology and provides considerable system performance gains. Before industrialization, there are still many open issues that need to be studied. We list the three most discussed issues in academia:

(1) Design and modeling theory of device unit. The RIS device unit used for communication needs to support dual-polarized incident signals, and have similar amplitude and phase response characteristics for dual-polarized incident signals. The design of the RIS device unit needs to design smart hardware that meets the requirements of the communication system from two aspects: device material selection and device structure. In the theoretical analysis, the RIS device unit is modeled as an ideal reflection unit, but the response signal parameters of the actual device unit are affected by many factors, such as incident signal angle, outgoing signal angle, and incident signal polarization direction. The accurate and efficient signal response model of the device unit is the basis for the performance evaluation of RIS.

(2) Channel modeling of RIS. A large number of RIS devices may be deployed in the future communication environment. The RIS cannot be abstracted as a simple communication node, and the existing wireless communication channel model is not suitable for channel modeling of the RIS. The academia needs to analyze and model the channel characteristics between the RIS and the base station or terminal node and perform testing and verification. In particular, the channel characteristics of the RIS are affected by the deployment of base stations, terminals, and RIS. System

simulation requires spatial modeling of RIS to accurately evaluate system performance.

(3) Channel measurement and feedback mechanism. Since the RIS is composed of a large number of device units and does not have radio frequency and baseband processing capabilities, the base station cannot obtain the channel information from the base station to the RIS as well as the channel information from the RIS to the terminal respectively. The received signal of the base station or the terminal is formed by superimposing the response signals of a large number of RIS device units. Changing the working state of one or a small number of device units cannot cause significant changes in the received signal. A possible measurement scheme [20] is to install a small number of active device units in the RIS, so that the RIS can actively perform channel measurement and feedback;The base station uses compressed sensing or deep learning algorithms to calculate reasonable RIS configuration parameters from the channel information. Communication systems based on RIS require an efficient channel measurement mechanism to improve the end-to-end signal quality as much as possible while ensuring the low complexity of RIS.

In addition, theoretical performance analysis of communication systems based on RIS, multi-user MIMO performance analysis, and exploration of RIS application deployment scenarios are also important aspects of subsequent research.

3.3.2 Distributed MIMO

In 2010, Professor Marzetta of Bell Lab proposed a large-scale antenna array which can be used in a base station to form a large-scale antenna system to greatly increase the capacity of the system. Thus, the theory of antenna technology is created. After the large-scale antenna technology was proposed, it immediately became a hot spot in academia and industry and was listed as a key technology for 5G. After ten years of development, large-scale antenna technology has been standardized in the 5G new air interface, and large-scale commercialization has truly begun. From the perspective of network deployment, large-scale antenna systems can be deployed in a centralized or distributed deployment. Distributed deployment can be traced back to

earlier distributed antennas, coordinated multi-point transmission and distributed MIMO (D-MIMO). Specifically, LTE-A standardizes the coordinated multi-point transmission technology, which can support cooperation between 2-3 base stations; The first version of 5G NR also supports coordinated multi-point transmission technology. The supported technical solution is dynamic transmission point selection; Rel-16 further supports non-coherent joint transmission (NC-JT). In general, for the previous version of the distributed deployment solution, there has a small number of base stations participating in cooperation, and it supports mainly incoherent joint transmission. Therefore, D-MIMO will be greatly enhanced in terms of the number of cooperative base stations and the transmission scheme.

D-MIMO fundamentally departs from the cellular paradigm by spreading out service antennas geographically over a large area, see Fig. 3.20. With D-MIMO, theoretically, all antennas participate in the service of every user terminal through phase-coherent beamforming. In practice, only the closest antennas will effectively contribute and be used.

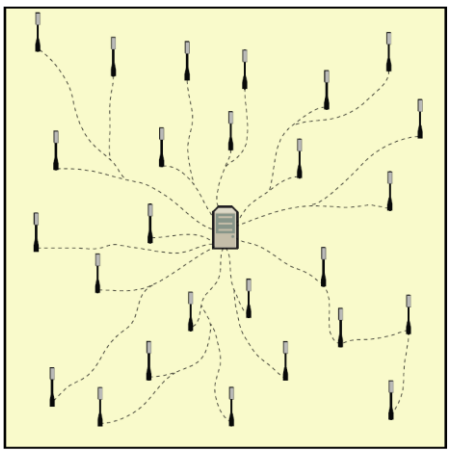

Fig. 3.20 Illustration of distributed MIMO with many distributed antennas

In the D-MIMO system, the chance is high that several of the antennas provide good channel conditions to a user and the risk of many distributed antennas simultaneously blocked is low; The short propagation distances enable reduction in transmit power, leading to higher energy efficiency. The service antennas are connected to central processing units, and payload data is shared between the access points. Short-term channel state information needs not be shared to perform coherent

beamforming, as long as the access points are synchronized. Therefore, D-MIMO architecture can result in order-of-magnitude improvements in quality-of-service, particularly measured as the 99%-likely performance. Moreover, D-MIMO is easier to support multi-stream transmission due to the low correlation between antennas. In the Rel-16 NR stage, in order to increase the transmission rate of edge users, a non-coherent transmission mechanism for eMBB scenarios is designed, and the low correlation between spatially separated antennas is also used to improve the probability of multi-stream transmission.

1. Use cases

In an airport or station with many moving users carrying wirelessly connected devices. The conventional way to cover such an area with communication services is to deploy access points (base stations) at distinct locations along the hallways and rooms, which are operated as small cells. Most of the time, each user will be in-between access points and experience mediocre data rates, due to interference and frequent blockage of the signals. For high-accuracy positioning, a similar issue is observed. Therefore, D-MIMO can supply a new idea to solve these problems. D-MIMO takes the communication performance to entirely new levels, in terms of reliability and uniformity of data rates.

Firstly, horizontally long, but vertically narrow, D-MIMO antenna unit can be hidden into the existing building blocks. Each user will be always physically close to one antenna unit, which can serve the user by coherent beamforming. Even if the nearest segment of the surface is blocked, the entire surface will never be blocked, leading to a reliable physical layer with only minor fluctuations in service rate and no outages. The short distances enable spatial multiplexing of many terminals per m2 and the use of extremely low transmit powers.

Secondly, the massive amounts of data collected on the physical layer by large antenna arrays open new possibilities for large-scale environmental perception, sensing and positioning. This is especially true when large coherent edge-processing is implemented through D-MIMO.

Use cases include mobility prediction, detection and tracking of moving objects, guarding against intrusion in protected spaces, remote health monitoring, and gesture recognition. It is already known that, for example, counting the number of persons in a room is possible with WiFi technology with relatively simple algorithms.

2. The challenges

Frequency offset: In actual products, each RRU uses a high-precision crystal oscillator, and uses the corresponding distributed node synchronization technology. However, due to the inconsistency of the radio frequency link, the air interface signal of each RRU still has a certain frequency deviation relative to the carrier frequency. The channel obtained through sounding signal is not only changed by the fading of the channel itself, but also changed by the frequency offset introduced by RRU, therefore the precoding matrix obtained by the precoding algorithm cannot effectively eliminate the interference in the cooperative cluster, thereby affecting performance.

Channel estimation error: Accurate channel estimation via reciprocity based on uplink sounding signals is important for precised scheduling and precoding. The traditional system only needs to estimate the channel from the user to the main serving cell, while the D-MIMO system needs to estimate the channel from the user to the cooperative node. The channel quality from UE to cooperating node is usually worse than that to the main serving cell, which further affects the accuracy of channel estimation.

Calibration error: D-MIMO need to solve the channel calibration between distributed nodes. Since the accuracy of air interface calibration algorithm depends on the channel quality of the calibration signal transmission link between the nodes or UE-assisted and calibration period, internal channel changes of D-MIMO bring challenges to the calibration accuracy. Thus, the detection accuracy of the calibration signal and the channel change during the calibration period pose challenges to the calibration accuracy for D-MIMO system.

Complexity: D-MIMO have the characteristics of a significant increase in the number of antennas, which brings a significant increase in complexity to the implementation of algorithms such as precoding and user pairing for distributed nodes.

Interaction delay and quantization error: Since frequent information interaction between nodes is existed in D-MIMO system, performance of D-MIMO system relies on the timeliness and accuracy of information interaction between nodes. Thus, improvement of interaction delay and quantization error becomes a great challenge to the actual D-MIMO system.

3.3.3 New signal processing

1. Transform domain precoding (TDP)

Due to the availability of wide bandwidth, high frequency band is promising for 5G evolution and 6G. With the increase of antenna ports and bandwidth, existing subband-level precoding in 5G NR consumes high feedback overhead and restricts the precoding granularity. However, channel sparsity can be observed in transformed angular-delay domain in mmWave systems with massive antennas. To utilize the channel sparsity in transform domains, a transform domain precoding (TDP) in practical system with hybrid beamforming and frequency domain windowing is proposed to design precoder and feedback [21].

Consider a downlink mmWave OFDM system with N subcarriers, where one BS equipped with M transmit antennas serves one single-antenna UE, i.e., MISO system. Channels in spatial-frequency domain can be transformed into angular-delay domain by two-dimensional DFT-FFT transformation.

Thanks to characteristics of multi-path channels in mmWave massive MISO systems, large-dimensional channels in space-frequency domain can be represented by small number of parameters in angular-delay domain. Due to limited scattering environments, channels in angular-delay domain are sparse as shown in Fig. 3.21.

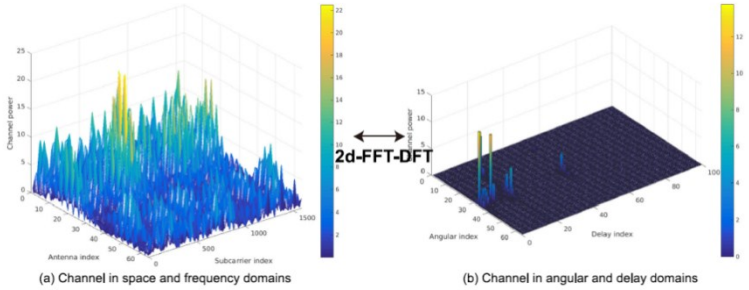

Fig. 3.21 Channels power (in linear scale) in various domains

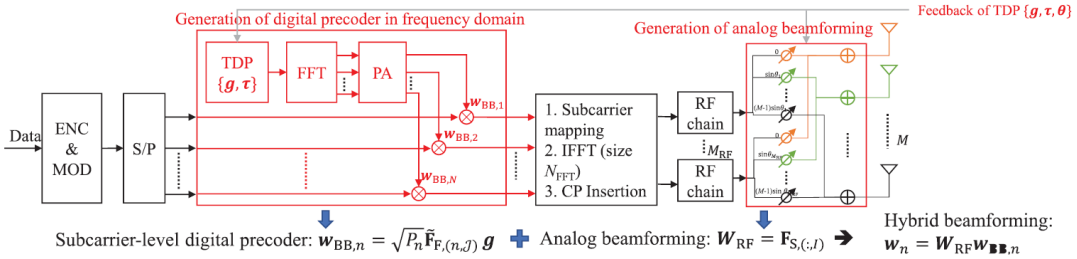

Fig. 3.22 Transmitter structure of TDP

Motivated by channel sparsity in transform domains, precoders should also be designed in transform domains to reduce the design complexity and feedback overhead. The transmitter structure of TDP is illustrated in Fig. 3.22, which is consistent with the hybrid beamforming structure in mmWave systems.

TDP is composed of three parts, i.e., angles, delays and corresponding coefficients. The hybrid beamforming at *n*-th subcarrier is obtained from TDP parameters, which can be optimized to maximize spectrum efficiency (SE) in allocated *N* subcarriers.

Due to the discrete-time signal processing, quantized angles and delays are used in TDP, which results in an integer optimization problem. To solve this problem, greedy searching algorithms in compressed sensing (CS) techniques, e.g., orthogonal matching pursuit (OMP), can be used.

Link-level simulations results in Table 3.2 and Table 3.3 show that 60%~89% overhead reduction and 2.38%~21% SE enhancement can be achieved by the proposed TDP, respectively.

Table 3.2 Overhead reduction of TDP at same performance

UE Bandwidth	50 RBs	100 RBs	150 RBs
Gain over Type I CSI with flexible number of subbands [2]	68%	84%	89%
Gain over space-delay precoding with flexible Q [3]	60%	60%	60%

Table 3.3 SE gain of TDP with Q=2 at same overhead (16bits)

SNR	-20 dB	-10 dB	0 dB	10 dB
Gain over Type I CSI with 8 subbands [2]	21%	14.3%	8.46%	4.06%
Gain over space-delay precoding with Q=2 [3]	8.13%	5.55%	3.73%	2.38%

2. Orbital angular momentum (OAM)

OAM is another important physical quantity besides the strength of electromagnetic waves. It provides another dimension for electromagnetic waves besides frequency, phase and space. The OAM multiplexing technology uses different orthogonal OAM modes to transmit multiple signals at the same frequency to achieve the improvement of spectrum efficiency and channel capacity.

When a phase rotation factor is added to the normal electromagnetic wave, the phase wavefront will no longer be a planar structure, but will rotate around the beam propagation direction. The physical feature of OAM makes the isophase plane of

electromagnetic waves spiral in the direction of propagation, and the phase changes by 2πl for one rotation. The intensity of the field strength at the center of the wavefront is zero. Electromagnetic vortex waves with different eigenvalues are orthogonal to each other, therefore OAM vortex waves with different eigenvalues can be transmitted in parallel within the same bandwidth. Common methods to generate OAM wave are: uniform annular array, spiral phase plate, spiral parabolic antenna and cyclic traveling wave antenna. The propagation of vortex electromagnetic waves has three major features: hollow, divergence and phase rotation.

In 2018, NTT, one of Japan's three major operators, announced that by combining OAM multiplexing and MIMO technology, 100Gbps transmission demonstration with a distance of 10 meters is realized at frequency of 28GHz, which is a breakthrough in Tbps wireless transmission. In the future, OAM multiplexing is expected to be combined with ultra-large-scale antenna systems to build a larger-scale uniform circular array (UCA) to further improve its spatial multiplexing gain, in the fronthaul/backhaul link, D2D and other near-field communications scenarios.

Major advantages：(1) Orthogonality. With the orthogonality between the various OAM modes, multiple independent and non-interfering signals can be simultaneously transmitted in the same frequency band, which will increase the achievable rate of the wireless communication. (2) Security. When multiple modes transmit at the same time, the OAM state can be directly detected only when the OAM wave is completely received. Angle offset and partial reception will spread the power of the transmission mode to other modes, reducing the detection rate of the OAM state Therefore, OAM-based multiplexing communication can effectively prevent eavesdropping.

Major challenge: Beam spreading and the limited gain in long-distance communication are two major challenges of OAM. As shown in Fig. 3.23, affected by the helical phase factor, the OAM electromagnetic wave will propagate in a helical shape so that the power of the signal is dispersed in the propagation space. For long distance transmission, a larger-scale antenna array is required to complete the signal reception, so it is necessary to design a spatially convergent OAM waveform to reduce the volume of the receiver. In addition, OAM multiplexing is naturally a special case of MIMO. As shown in Fig. 3.23, when the propagation distance is larger than the Rayleigh distance, the gain of freedom degree brought by OAM multiplexing will reduce accordingly. Therefore, it is necessary to study how to effectively increase the Rayleigh distance of the OAM beam to achieve long-distance high-speed

transmission.

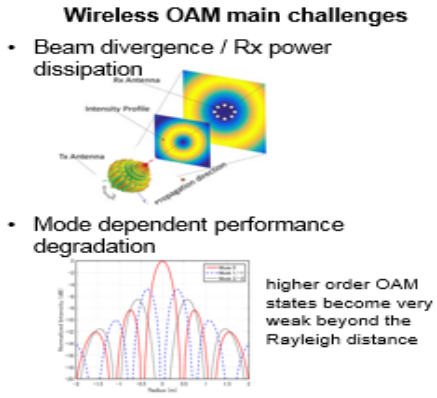

Fig. 3.23 Challenges of OAM multiplex

3.3.4 New application

1. Multi-dimensional Positioning

The traditional MIMO technology has limited applications in wireless positioning due to the limitation of the antenna scale. With the development of Massive MIMO technology, its potential in positioning is gaining increased attention. In traditional time-based positioning systems, the position accuracy is correlated with SNR and bandwidth. The future 6G communication system will continue to increase the antenna scale and communication frequency, and it is expected to realize the detection of user equipment's orientation (such as roll angle, pitch angle, and yaw angle) based on three-dimensional positioning in space. As shown in Fig. 3.24, the antenna array on the base station side can detect the angle of arrival (Angel of Arrival, AoA) and angle of departure (Angel of Departure, AoD) of the user's uplink or downlink signal to complete the user's two-dimensional positioning. When the user is equipped with an antenna array, the system can simultaneously detect the user's AoA and AoD in the uplink and downlink, and finally estimate the user's heading parameters to achieve multi-dimensional positioning. Achieving high-precision positioning is of great significance in indoor application scenarios such as industrial robots, games, social networks, and virtual/augmented reality.

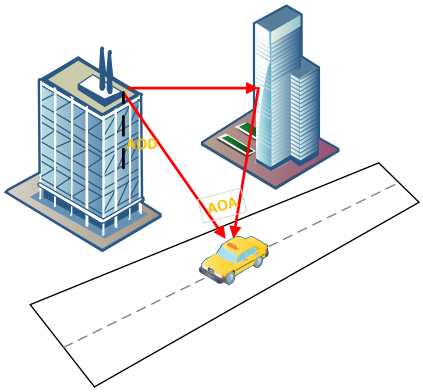

Fig. 3.24 Multi-dimensional positioning based on extreme MIMO

Major challenges: The positioning performance is limited and integrated heterogeneous positioning methods are required. Communication and positioning have mutual influence. The channel environment suitable for communication is not necessarily beneficial to positioning. It is necessary to realize the integration of communication network and positioning network in the architecture level, and study how to add appropriate positioning manage and synchronize nodes to the existing mobile communication networks. At present, there is no positioning technology which can meet the requirements of indoor and outdoor coverage and positioning accuracy at the same time. The positioning technology based on satellite navigation system is widely used for outdoor positioning, but for indoor scenario satellite signals are easily blocked and the accuracy is limited. The mainstream positioning technology generally has the shortcomings of small coverage and high cost. The future positioning system needs to include different positioning technologies and realize the intelligent combination of various technologies at the same time, including joint signal measurement, joint position estimation algorithm, joint positioning decision and feedback.

3.4 Holographic radio (HR)

Holographic radio is a full-dimensional coherence in space-time-frequency domain, and a linear coherence described by Fourier Transformation. There are three main characteristics of the HR-based 6G communication system:

(1) fully closed loop control: The traditional abstraction of the channel state using simplified modelling and less feedback (especially at higher carrier frequencies) is not sufficient. This is because an over-simplified model is usually not capable of

emulating unknown channels. Therefore, a paradigm shift will be necessary for the closed-loop feedback on exactly emulating channels.

(2) interference exploitation: A dense network with a smaller cell size and an increase in the number of antennas (such as massive or extreme MIMO) corresponds to a commensurate increase in intra-cell and inter-cell interference. Although the use of massive MIMO in 5G can use simple linear operations to eliminate interference, beamforming design usually strikes a trade-off between canceling interference and maximizing the signal to interference plus noise ratio (SINR). Therefore, traditional interference cancellation techniques are no longer optimal, and innovative methods of exploiting interference are emerging. In contrast to the traditional view that interference is regarded as a harmful phenomenon, HR-based 6G will exploit interference as a useful resource for the development of energy-efficient, high-precision holographic communication systems.

(3) photonics-defined system: The next generation of 6G systems will have higher carrier frequencies for smaller antennas and broadened bandwidth for increased resolution. A significant challenge for future radio systems will be to instantaneously analyze and process RF signals over an extremely broad bandwidth of 100 GHz or more in real time and without any prior knowledge of the signals, carrier frequency, and modulation format. The photonics-defined system can provide extremely high broadband and even full spectrum capacity, so it will become an ideal platform for 6G future radio.

Unlike traditional massive MIMO, HR uses Fresnel-Fraunhofer interference, diffraction, and spatial correlation models instead of traditional Rayleigh propagation models to model and compute holographic radio space. Accurate computation of communication performance requires detailed electromagnetic numerical computations, that is, algorithms and tools related to computational electromagnetics and computational holography, instead of ZF, MRC and MMSE in mMIMO. Generally, spatial correlation propagation model is described based on Fresnel-Kirchoff integral. Moreover, HR uses holographic interference imaging to

obtain the RF spectral hologram of the RF transmitting sources (UEs), not requiring CSI information and channel estimation. At the same time, a 3D constellation of distributed UEs in RF phase space can be obtained through spatial spectral holography, providing precise feedback for spatial RF wave field synthesis and modulation in the downlink. Spatial RF wave field synthesis and modulation can obtain a 3D pixel-level structured electromagnetic field (similar to an amorphous or period electromagnetic field lattice) which is the high density multiplexing space of HR and different from sparse beam space of mMIMO. On the other hand, spatial correlation can covert multiple path signals to background noise which will be cancelled in mMIMO signal processing, instead holographic radio exploits interference by spatial correlation. Thus, HR is the technology with the most potential and highest level of interference exploitation.

In general, the HR technology can achieve holographic imaging level, ultra-high density and pixelated ultra-high resolution spatial multiplexing. Fig. 3.25 shows the main difference between the HR and the conventional massive MIMO. It has the key features in terms of fully closed loop control, interference exploitation and photonics-defined system, which are should be built on heterogeneous optoelectronic computing architecture, seamless integration between photonics-based continuous-aperture active antenna and high-performance optical computing. In addition, meta-surface aided HR, and convergence of imaging, positioning, sensing as well as communication over HR will show a more promising mobile network.

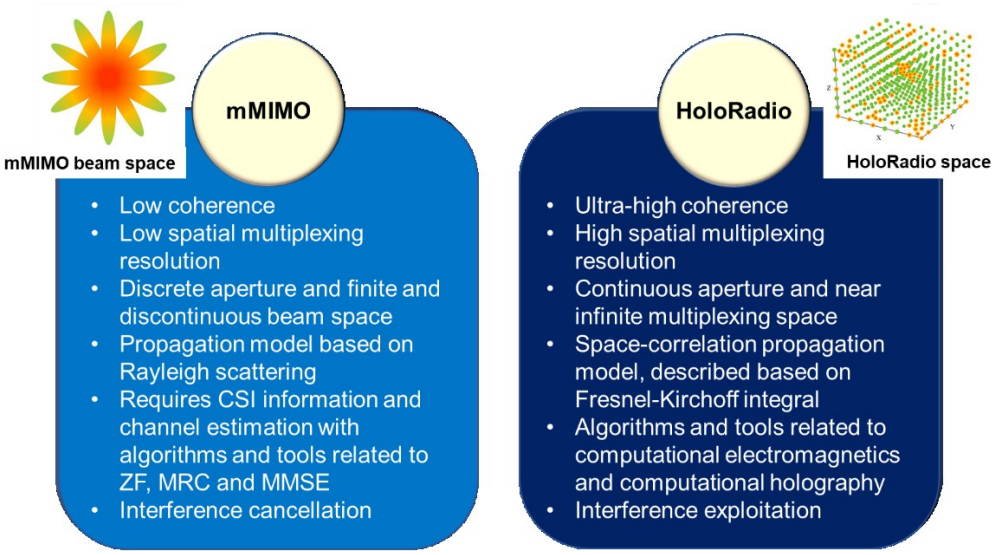

Fig. 3.25 mMIMO beam space vs. holographic radio space

3.5 Multi-dimensional networking

3.5.1 THz communication

In the future 10 years, new applications will continue to develop and new 6G applications such as AR/VR/XR, industrial automation, and brain-computer interconnection put forward requirements for large capacity, higher data rate and lower latency. Low-frequency spectrum resources are insufficient to support future communications and how to meet the demand for capacity is an important research direction for 6G. The availability of continuous large bandwidth in terahertz band can provide a data rate of up to Tbps to meet ultra-high throughput, low delay and brand-new 6G application scenarios.

Terahertz refers to the frequency band resource of 0.1-10THz, which has a large amount of unexploited spectrum and is considered as the last unused spectrum resource, that is, Terahertz Gap. The terahertz technology provides abundant spectrum resources, and is regarded as a basic technology meeting the 6G KPI indicator. It plays an active role in improving the peak rate, user experience rate, spectrum efficiency, energy efficiency, number of connections, reducing latency and supporting mobility. Terahertz has many superior properties, such as low time-domain SNR, strong absorption and resonance for biological macromolecules, ability to penetrate

objects such as cloth, large bandwidth and high time-domain resolution. At the same time, terahertz exhibits unique characteristics, such as high path loss, molecular absorption and serious scattering, posing many new challenges to the implementation of Tbps links.

The main objectives of the terahertz communication technology include: ultra-high data rate and reasonable transmission distance of a single device, regional ultra-high throughput and ultra-large number of connections, ultra-reliable connections to support various key applications in the mobile environment, and ultra-high energy efficiency to support various terminals and networks. The terahertz application involves wireless cognition, sensing, imaging, wireless communication, positioning, navigation and so on. The ultra-wideband spectrum makes it possible for real-time calculations of human cognition during wireless migration. The frequency selective resonance, material absorption and small-scale antennas can be used to achieve terahertz sensing. The features that being less affected by the weather and ambient light make terahertz imaging more effective. The high frequency characteristics of terahertz make centimeter-level positioning possible, and the combined use of sensing, imaging and positioning can reconstruct a three-dimensional map of the unknown environment. The ultra-high bandwidth of terahertz can support high-speed data transmission and MU access. The combination of terahertz frequency band with sub-6G and millimeter wave is an inevitable trend for 6G network in the future.

According to the current academic and industrial requirements, terahertz communication supported application scenarios include large-scale scenarios such as large-capacity wireless fronthaul/backhaul, wireless data centers, car networking, inter-satellite links, small-scale scenarios such as 6G cellular networks, WLAN, WPAN and nano-scale scenarios such as high-speed short-distance point-to-point communication, health monitoring, nano-scale IoT and chip communication. Additionally, terahertz also has various extended applications in vertical industry, for example, non-destructive detection in industrial application, detection of contraband

in security applications and detection of hazardous ingredients in food safety applications.

To make better use of terahertz frequency band resources, the research contents we face include measurement and modeling of terahertz channels, R&D of hardware devices, research on baseband processing algorithms and integration of terahertz and other technologies. The following describes the detail.

Compared with the low frequency band, the terahertz channel has the characteristics of large transmission loss and severe molecular absorption. There are multiple atmospheric absorption peaks, forming multiple atmospheric windows, and the water vapor absorption is severely attenuated, causing the transmission distance to be limited. It is necessary to specially design transmission strategies for different spectral windows and use extremely narrow directional beams to overcome path fading and extend the propagation distance.

During the propagation of terahertz which has short wavelength, the probability of scattering increases greatly and the energy of the scattering path dominates as the frequency increases. How to establish a proper propagation model to represent terahertz channels with high-precision and low-complexity is an urgent problem to be solved. It is necessary to make full use of the sparse characteristics of terahertz channels for low-complexity modeling and estimation, and overcome the channel dimension increasing problem caused by multi-antennas. Research on how to model and use scattering paths, enhance the energy of received signals, and overcome the path blocking problem are needed.

Terahertz devices are the main restricting factor for the development of terahertz technology. The photonics based terahertz communication system can achieve high transmission rate and high bandwidth utilization. However, the transmission power is only in microwatt-level with large system and high power consumption. The integration remains a severe challenge, making it inapplicable for remote space information networks and mobile systems. The electronics based system has the characteristics of small size, easy integration and low power consumption, but the

phase noise deterioration of the local oscillator after multiple frequency multiplications is serious and difficult to overcome. The direct modulation THz communication system is easy to integrate, small in size and flexible, but it is difficult to directly modulate at high speed and the related research is far from complete.

As for terahertz hardware IC, CMOS technology has limited operating frequency and output power and it is necessary to explore new III/V semiconductor technologies such as silicon germanide and indium phosphide. The future research direction of terahertz integrated circuits is to process the accurate nonlinear modeling and parameter extraction of high-frequency semiconductor devices, design broadband impedance matching THz circuits to improve the efficiency, overcome the limitations of small processing size, high precision requirements and processing error sensitivity of cavity.

For terahertz ADC/DAC, the signal bandwidth of terahertz high-speed communication is extremely wide and the sampling rate of the current sampling chip cannot meet the requirements, which emphasizes the importance of breaking through of high-speed sampling and chip implementation. As for the design of terahertz antennas, electronic terahertz radiation sources are the most concerned one but still cannot meet the requirements of industrial applications. The development of new materials for solid devices is needed to promote the performance of electronic radiation terahertz sources. Heterodyne signals in optical terahertz radiation sources have a bright prospect, though its energy conversion efficiency needs to be improved to operate at room temperature. In the future, it is necessary to find new nonlinear materials, explore new mechanisms such as terahertz radiation, oscillation and amplification, as well as promote the rapid development and integration of related traditional disciplines and interdisciplinary disciplines.

Terahertz communication needs to deal with ultra-large bandwidth, ultra-high-speed data transmission, and handle large path loss, serious time expansion, spectrum window changes, large delay propagation, frequent synchronization, carrier frequency deviation and serious phase noise, etc. Waveform design, modulation

coding, synchronization, and beam management should be carefully designed to adapt to these features.

For waveform design, the single carrier scheme is simple to implement with low hardware cost and better PAPR performance, thus attracted great attention. The multi-carrier scheme can solve the multi-path expansion and is robust to narrowband interference, promising a broad application prospect. Modulation and coding design needs to adapt to high frequency characteristics, improve cell coverage, cope with frequent synchronization and overcome the influence of phase noise. Low PAPR methods and those that overcome and compensate for high phase noise are more concerned. For beam management, beam training should quickly find ultra-narrow beam links that meet transmission conditions with low training overhead, delay and complexity. For beam tracking, the used ultra-narrow beam links must be adjusted and switched rapidly. For beam recovery, new ultra-narrow beam link should be rapidly re-established when the original beam link fails.

As a new frequency band resource, terahertz has its unique advantages and the integration of terahertz and other promising technologies can give full play to its advantages. The combination of terahertz and massive MIMO makes it possible to integrate a massive number of antennas in a small footprint, forming extremely narrow beams with high directivity. In this way, the severe path loss can be compensated and the transmission distance can be extended. The combination of terahertz and reconfigurable intelligent surface make the transmission controllable and form an intelligent wireless environment, solving the problem that terahertz communication is easily affected by the environment which causing communication interruption. The combination of terahertz and orbital angular momentum can improve channel incoherence and overcome the beam divergence of OAM. It can increase system capacity, solve the problem of limited single-user multiplexing layers under high-frequency LOS channels and achieve higher spectrum efficiency.

3.5.2 Cross-media relay and cooperation

Since the end of the 19th century, when the feasibility of radio frequency

transmissions was confirmed, mankind has developed to realize the dream of perfect wireless multiple media communication, meeting people to communicate with anyone, anywhere, at any time, using a sequence of multimedia services. With the development of B5G/6G mobile communication system, the requirements in terms of service quality such as the achieved rate, latency, transmission power consumption/allocation are higher. Moreover, there will be more scenarios where a massive number of receiver devices working in various multiple media accompanied by the rapid development of the wireless communication.

However, optical-and quantum-domain wireless communications is less developed than radio frequency wireless communication. To satisfy the demand of such scenario where a mass of devices working in different media, only radio frequency wireless communication technologies are not enough. It is obvious that the requirement for the large data volume and ultra-high speed of B5G/6G mobile communication will not be satisfied by only developing radio frequency wireless communication technologies. Thus, it is urgent to find a promising candidate of the associated environment al and financial benefits to achieve the large data volume and ultra-high speed. International Telecommunication Union (ITU) suggest some new candidate bands for 5G communication. Among them, optical band is supposed to be a more promising answer for the large data volume and ultra-high speed from an economic and environmental perspective. Especially, visible light communication (VLC) techniques presented many advantages including cheap transmitters and receivers, low power consumption and good safety features. Integrating VLC with radio frequency-based wireless networks has improved the achievable date rate of communication link.

A simple cross-media scenario is considered to explain the proposed system in Fig. 3.26, which the base station has multi-media capabilities that allow simultaneous transmission to the two receivers D_1 and D_2 working in different media. For example, the medium between the base station and receiver D_1 is visible light, while the medium between the base station (denoted by S) and receiver D_2 is microwave. The system

model of the above scenario is shown as follow.

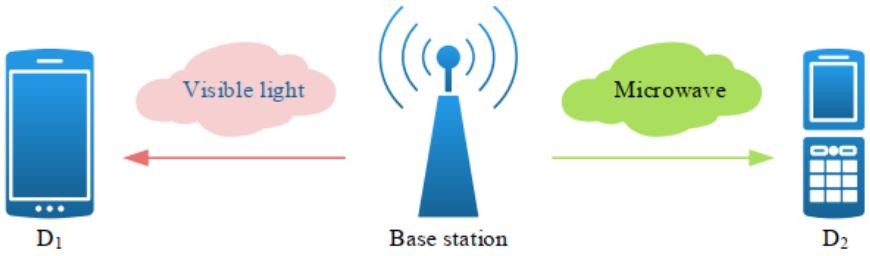

Fig. 3.26 System model of the proposed cross-media system

Consider the achieved rate from S to D_1 and D_2 working in different media in the long term, the minimum of $\left\{R_{S,D_1}, R_{S,D_2}\right\}$, denoted by $R_{\min}$, would be the data rate of the proposed cross-media system. Hence, two optimization criteria of the maximizing the minimum rate are formulated to maximize the average rate of the proposed cross-media communication system, which denoted by the criterion of Maximizing the minimum achieved rate and the Maximizing the Sum achieved Rate, respectively.

In Fig. 3.27 and Fig. 3.28, two optimization criteria of the maximizing the minimum rate are in comparison to the equal power allocation counterparts. Fig. 3.27 shows the minimum achieved rate in b/s versus the maximum transmission power of the BS to study the impact of increased transmission power in the cross-media communication system. It is observed that the minimum achieved rate increases with the increase of the maximum transmission power increasing under three schemes, which is denoted by 'Max-Sum', 'Max-Min' and 'Equal Power Allocation', respectively. As it can be seen, the minimum achieved rate of 'Max-Sum' and 'Max-Min' are higher than that of 'Equal Power Allocation'. It is noteworthy that the minimum achieved rate of and 'Max-Min' are higher than that of 'Max-Sum'. This is expected since with any increased transmission power, BS can allocate more power on weak communication link to obtain high achieved rate based power allocation and bisection algorithm. Fig. 3.28 illustrates the effect of the value of d_{S,D_1} on the minimum achieved rate for three schemes of the proposed cross-media communication system. As d_{S,D_1} increases, i.e., when the BS is near to D_2, the channel gain of Microwave communication link

becomes higher and the achieved rate increases. It is observed that the minimum achieved rate of 'Max-Min' outperforms that of 'Max-Sum' and 'Equal Power Allocation'. This is expected since with given total power, BS is forced to allocate more transmission power to improve the minimum achieved rate for the scheme of 'Max-Min'. In contrast, the scheme of 'Max-Sum' allocate more transmission power to obtain the maximum sum achieved rate.

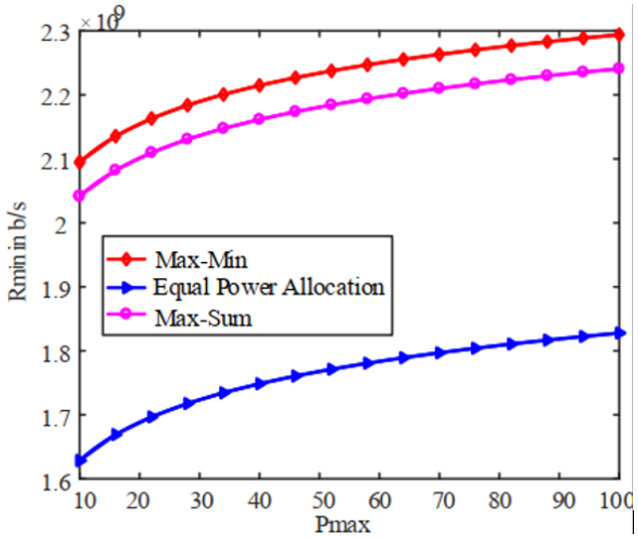

Fig. 3.27 The minimum achieved rate against the total transmission power of Base station

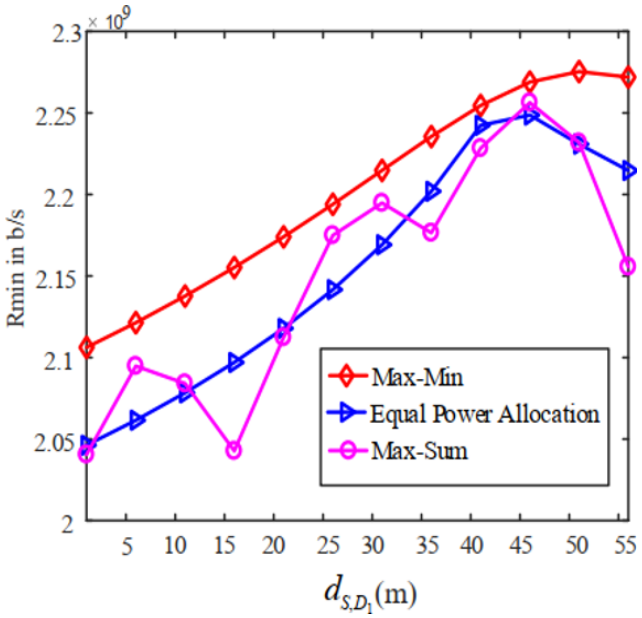

Fig. 3.28 The minimum achieved rate against the position of Base station

4 Air interface enhancement and reconstruction based on AI

4.1 Learning framework for wireless communications

4.1.1 Distributed learning for wireless communications and networking

With the fast development of smart terminals and emerging new applications (e.g., real-time and interactive services, distributed learning, IoT), wireless data traffic has drastically increased, and current wireless networks cannot completely match the quickly rising technical requirements. As a result, the expectation and development of next generation mobile networks, e.g., 6G, have attracted a great deal of attention. Recently, machine-learning based methods have been viewed as a key enabler for 6G, since the key issues behind synchronization, channel estimation, equalization, MIMO signal detection, iterative decoding, and multi-user detection in wireless communication systems can be solved by carefully designed machine learning algorithms. In addition to academy, standard body is also considering to include machine learning in future mobile networks. For instance, in Release 16, 3GPP has started to improve the data exposure capability to support data-driven machine learning.

To date, most existing machine learning approaches solutions for wireless networks require centralizing the training data and inference processes on a single data center. In other words, the collected data have to be first sent to a center server (or cloud) and analyzed and then the results are sent back to the actuators. However, due to privacy constraints and limited communication resources for data transmission in future networks, it is impractical for all wireless devices that are engaged in learning to transmit all of their collected data to a data center or cloud that can subsequently use a centralized learning algorithm for data analytics. To elaborate further, the centralized machine learning approaches have some inherent disadvantages that limit their practicality, such as significant signaling overhead, increased implementation complexity and high latency in dealing with communication problems. Moreover, emerging wireless networking paradigms, e.g., cognitive radio networks, ad-hoc networks, and D2D communications, are inherently

distributed. Furthermore, in the view of future applications, the centralized approaches may not be suitable for applications that require low latency, such as controlling a self-driving car or sending instructions to a robotic surgeon. To perform these mission-critical tasks, future wireless systems must make more quickly and reliably decisions at the network edge.

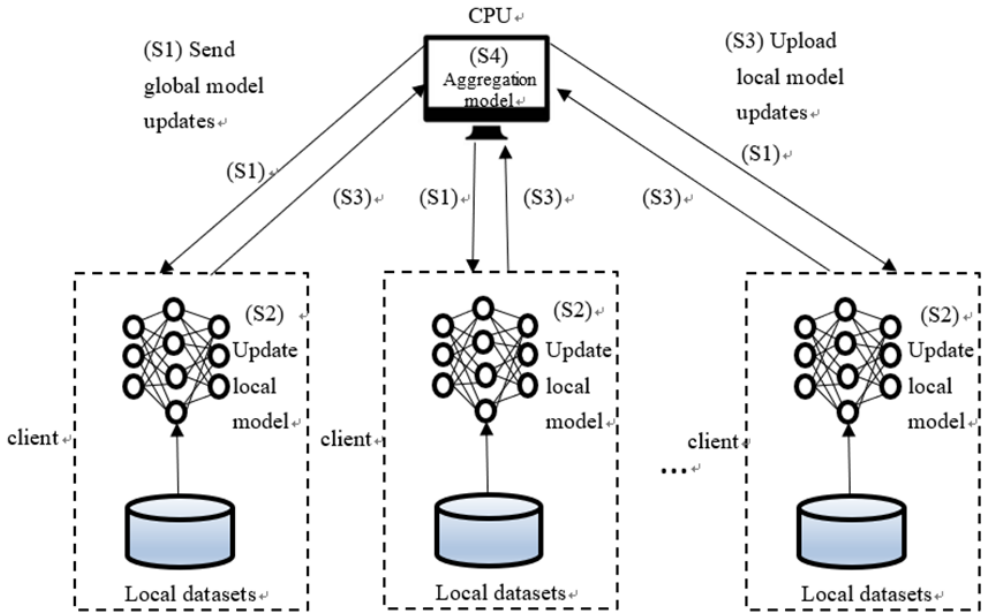

Fig. 4.1 Federated learning model

To solve this massive scalability challenge while addressing privacy, latency, reliability and bandwidth efficiency, distributed learning frameworks, e.g., distributed gradient descend, alternating direction method of multipliers (ADMM) and federated learning (FL), are needed and intelligence must be pushed down onto the network edge in future wireless communications and networking. In these frameworks, mobile devices are capable of collaboratively building a shared learning model with training their collected data locally. Motivated by this appealing concept, numerous research activities in distributed machine learning were sparked. For example, FL has been proposed to enable users to collaboratively learn a shared prediction model while remaining their collected data on their devices for user behavior predictions, user identifications, and wireless environment analysis. Similarly, to increase robustness, ADMM is widely considered for large scaling distributed learning. Likewise,

distributed gradient descend methods are also widely studied for various potential applications. Specifically, FL is a decentralized distributed deep learning training framework, which can effectively improve the computational efficiency of the model and make reasonable use of data and resources. FL enables all clients to collaboratively learn a shared predictive model without uploading training data, while each client retains all its own training data without uploading the data to a central server for machine learning. The model of FL is shown in Fig. 4.1.

The FL process is an iterative process. First, the central server shares the initial global model to the client; then, the client computes updates to the current global model on its local training data and sends the updates to the central server; then, the central server aggregates these updates and computes the global training updates and sends them back to the client to further aid in the computation of its local model updates. The iterative process is terminated when a certain learning accuracy is reached.

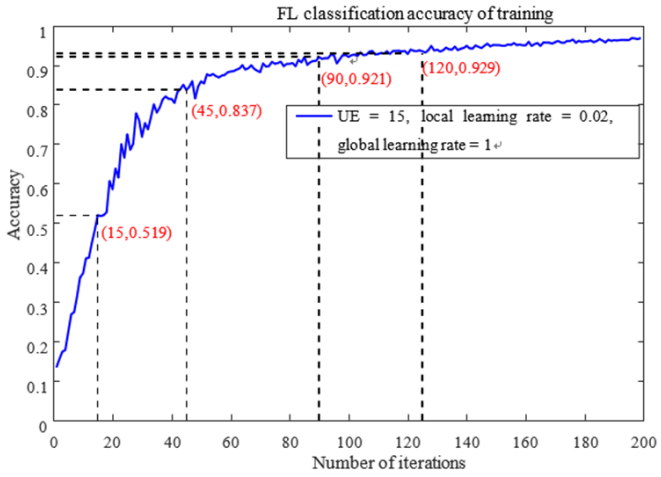

Fig. 4.2 The relationship between classification accuracy and number of iterations

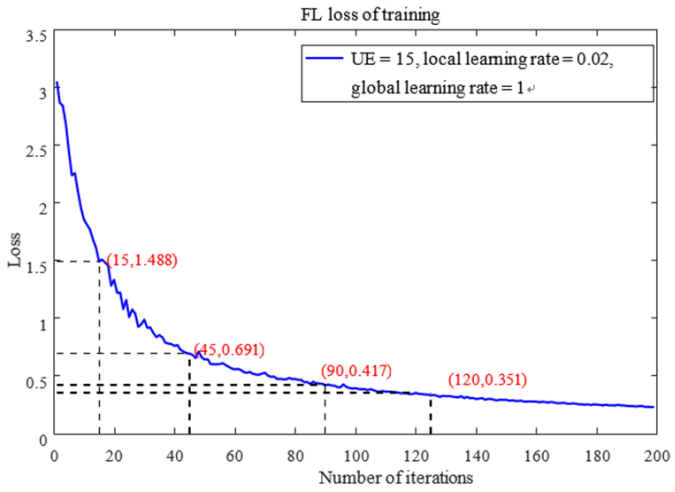

Fig. 4.3 The relationship between training loss and number of iterations

Fig. 4.2 and Fig. 4.3 compare the relationship between classification accuracy, training loss, and number of iterations when the system has 15 users and the learning rate is 0.02 for the local stochastic gradient descent optimization algorithm and 1 for the global stochastic gradient descent optimization algorithm. The data set for each user at each round of iteration will randomly select 20 images from the entire training set.

From Fig. 4.2, we can get the relationship between image classification accuracy and number of iterations. The classification accuracy improves quickly at the beginning of the iteration. After 15 iterations, the classification accuracy is 51.9%. After 45 iterations, the classification accuracy is 83.7%. The classification accuracy only improved by 31.8%. In this 15-45 iteration interval, the average classification accuracy improves by 1% per iteration. After 90 iterations, the classification accuracy is 92.1%. After 120 iterations, the classification accuracy is 92.9%. In this interval, after 30 iterations, the classification accuracy improves less than 1%; This indicates that the classification accuracy improves rapidly when starting iterations, and stabilizes after reaching about 97% as the number of iterations increases, and the 97% classification accuracy indicates that the training results are good.

The relationship between the number of iterations and training loss can be obtained from Fig. 4.3 as follows: the training loss decreases sharply at the beginning of the iteration, with a loss of 3.1 at the beginning of the iteration. After 15 iterations,

the loss is 1.488, a loss reduction of 1.612, with an average loss reduction of 0.1 per iteration in the 0-15 iteration interval, which is the fastest loss reduction in this interval; after 45 iterations, the loss is 0.691, a decrease of 0.797 compared to 15 iterations, and an average decrease of 0.027 per iteration in the 15-45 iteration interval, with a faster decrease in losses in this interval; 0.417 after 90 iterations and 0.351 after 120 iterations, with a decrease of less than 0.1 after 30 iterations in this iteration interval, the loss decreases slowly; after 120 iterations, the loss decreases the slowest and changes very little. It shows that as the number of iterations increases, the loss tends to converge.

However, the field of decentralized/distributed learning is still at its infancy as there are many open theoretical and practical problems yet to be addressed, such as robustness, privacy, communication costs, convergence, complexity, and how to optimally combine with physical layer transmission networks, etc. Given this situation, the following topics may be interesting for 6G Wireless Communications and Networking (WCN), including:

Category 1: Topics on novel distributed learning frameworks and theories for the physical layer.

(1) Distributed learning for beyond 5G multiple carrier and multiple antenna system design, including channel estimation and combing learning with detection and decoding;

(2) Distributed learning WCN with reconfigurable intelligent surfaces;

(3) Designs of ADMM, multiple agent reinforcement learning and federated learning for novel WCN applications and service scenarios;

(4) Fundamental performance metrics and limits of distributed learning WCN, e.g., convergence rate, power efficiency, hardware cost, computational complexity, and privacy and their tradeoffs;

(5) Testbeds and experimental evaluations of distributed learning WCN.

Category 2: Topics on distributed learning for the media access layer and the network layer

(1) Network architectures and communication protocols for energy efficiency/ultra-low latency/private distributed learning WCN;

(2) Wireless network optimization/ radio resource management for distributed learning WCN;

(3) Multiple agent reinforcement learning with game theory for access;

(4) Network slicing based resource allocation and software defined net¬working (SDN) based applications;

(5) Distributed learning edge caching and offloading, joint computation and communication resource allocation.

Category 3: Topics on the integration of other advanced emerging theories and techniques with distributed learning in mobile networks

(1) New deep learning architectures for distributed learning WCN, e. g., demystifying parallel and distributed deep learning, private distributed deep learning, and Gossip learning;

(2) Use of block chain/tensor optimization/big data /age of information/quantum computation for distributed learning WCN;

(3) Co-design of data compression/quantization and distributed learning for WCN.

These researches can be viewed as an interdisciplinary branch of intelligent wireless communications, which involves intelligent digitization, processing and recognition technique of wireless network. Moreover, in the training based distributed learning, e.g., neural networks, the methods in advance data mining and high-performance computer science will be included.

4.2 Air interface enhancement and reconstruction: Use case studies

4.2.1 AI based channel estimation

Accurate estimation and compensation of the wireless channel can greatly improve the performance of the communication system. Some studies have shown that wireless communication physical layer technology can be combined with deep learning to improve physical layer performance or reduce complexity. This solution

focuses on the combination of deep learning and DMRS-based channel estimation, using deep learning algorithm to replace traditional channel estimation algorithms. And algorithms performance and generalization capability are verified at the end.

Traditional channel estimation algorithms include LS (Least Square) algorithm, MMSE (Minimum Mean Square Error) algorithm, LMMSE (Linear Minimum Mean Square Error) algorithms and so on. The former LS algorithm does not consider noise and has poor performance, while the MMSE and LMMSE algorithms involve matrix inversion and have high complexity.

This solution uses deep learning algorithms instead of traditional algorithms. The input of the network is the channel information linearly interpolated based on the channel information of DMRS. The output of the network is the channel information of data and pilot. The theoretical of this solution is the traditional image super-resolution, regard the channel information after LS estimation as a low-resolution picture, and the channel information output of the neural network as a restored high-resolution picture. Therefore, the deep learning algorithm for image super-resolution can be used for channel estimation, such as SRCNN (Super-Resolution Convolutional Neural Networks) with only three convolutional layers, FSRCNN (Fast Super-Resolution Convolutional Neural Networks), EDSR (Enhanced Deep Super-resolution Network), etc. This solution is based on SRCNN and adds two convolutional layers.

The data set of this algorithm was generated based on Matlab platform. This simulation only considers the single-transmit and single-receive scenario. The input is generated after linear interpolation of the channel information of the DMRS, and the label is the perfect channel information, that is, calculated using the ideal Power-delay profile. The main simulation parameters are shown in Table 4.1.

Table 4.1 Simulation parameters

PRBs	51
SCS	30kHz
Symbols	14

DMRS configuration	F:A=1:1Note1，F:A=1:2
Tx and Rx antennas	1，1
Channel type	TDL-C
DelaySpread	$3 \times 10^{-7}s$
MaximumDopplershift	110Hz
Note1：F:A is Front-loaded DMRS : additional DMRS	

Firstly, we compare the performance between CNN algorithm and traditional algorithm. Fig. 4.4 shows the results when the number of PRBs is 51 and the SCS is 30 KHz. The horizontal coordinate is SNR (Signal Noise Ratio), the vertical coordinate is NMSE (Normalized Mean Square Error) in dB. Several baselines are also included: The Transform Domain CE in this simulation is the transform domain denoising interpolation algorithm, and the Ideal LMMSE is the LMMSE algorithm that the autocorrelation matrix is calculated based on perfect channel information to. Note that different networks are trained for different SNRs. It can be seen from Fig. 4.4 that the channel estimation accuracy increases when the SNR increases. And under the same SNR, the CNN algorithm is better than the LS algorithm and the Transform Domain CE algorithm. Therefore, the channel estimation algorithm based on deep learning has a better performance.

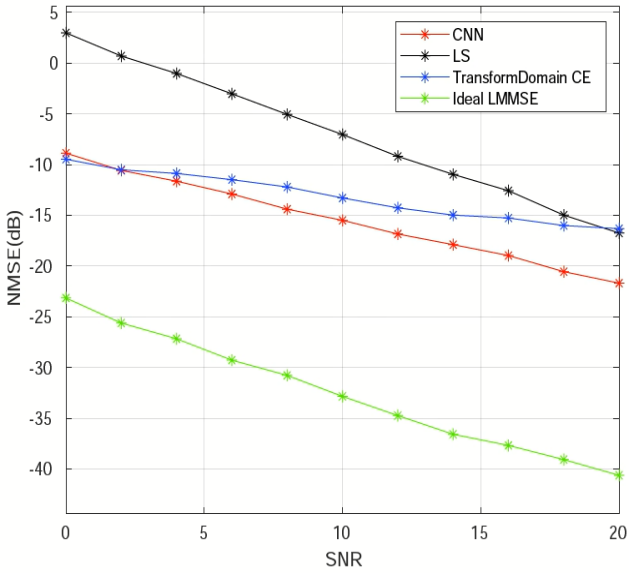

Fig. 4.4 Performance comparison between CNN algorithm and traditional algorithm

Next we concentrate on the generalization capability of CNN algorithm. Different value for channel parameters (delay extension, SNR, etc.) are set to verify the performance of the CNN algorithm. Both the training set and the test set are generated under the following channel parameter configuration, and the signal-to-noise ratio of the training set is randomly generated under the SNR of 0dB to 25dB. The following Table 4.2 presents the performance simulation results. From the results, after the generalization of some channel parameters, the CNN-based channel estimation algorithm still performs better than traditional algorithms. So it can cope with the changes of channel environment.

Table 4.2 Simulation result

DMRS configuration	Channel parameter	Simulation results
1 ： 1	DelaySpread = [200,300] ×10-9s MaximumDopplershift = [5, 100]Hz	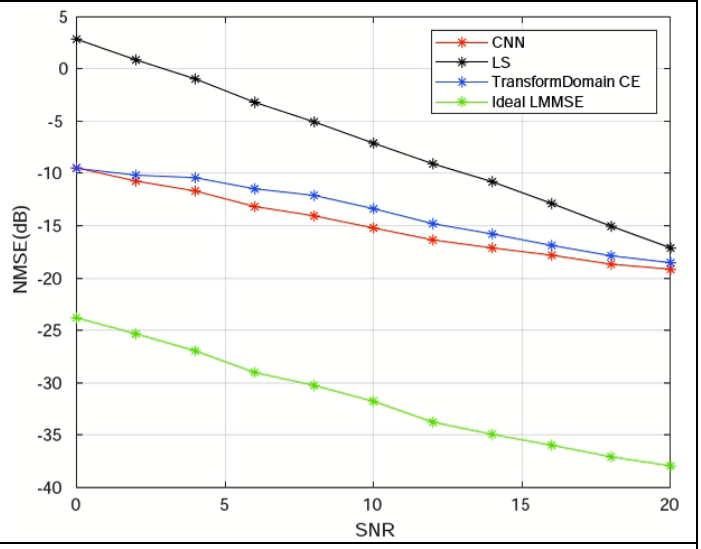
1 ： 2	DelaySpread = [200,300] ×10-9s MaximumDopplershift= [5, 400]Hz	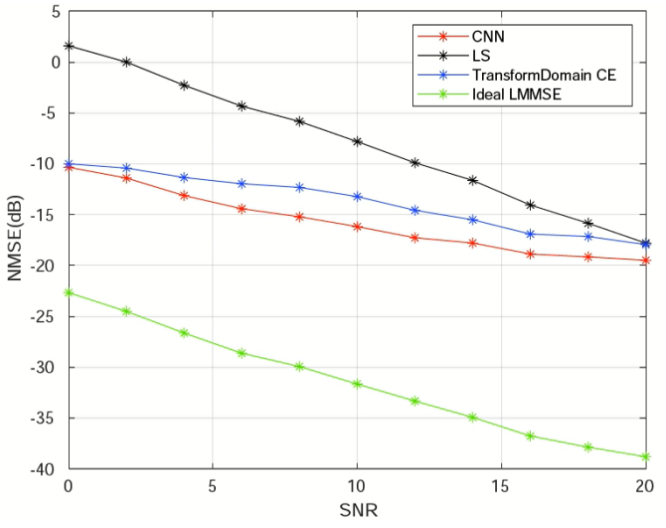

4.2.2 Channel state information feedback

Massive MIMO is considered to be a key technology for 5G system to meet the growing needs of the mobile data traffic, whose performance mainly depends on the effective channel state feedback and the matched channel coding mechanism. In order to fulfill these requirements, various of vector quantization and codebook-based CSI feedback methods are adopted in current 5G system, e.g. NR TYPE1 and TYPE2 CSI feedback[23][24]. Meanwhile, researchers from both academia and industry are looking for new approaches to gain the improvement of MIMO system, e.g. taking full channel feedback and AI based approaches into account, and numerous studies have achieved productive results [26-33]. Among these works, [27] as a pioneer firstly introduced image compression based techniques to massive MIMO CSI feedback and proposed a novel CSI sensing and recovering model known as CsiNet. After that, a series of follow-up studies have been carried out. Utilizing the CsiNet in the long-short time memory (LSTM) architecture by considering the temporal correlations of channel state is proposed in [27-30]. In addition, discussions on quantization have been conducted in[32][33] on the AI modules for quantization as well as dequantization.

In this section, further studies based on the CsiNet architecture will be discussed to analyze the performance gain between AI based approaches and the classical methods that are used in current 5G standards. A modified CsiNet model(described as CsiNet-Mode1) is proposed and applied to more practical scenario according to the channel assumption in 3GPP [25].

The considered system model is illustrated as follows: typical MIMO system with N_T transmit antennas at the base station and N_k receive antennas at UE side, carrier frequency 3.5GHz, carrier bandwidth 10MHz, subcarrier spacing 15kHz, basic feedback granularity every 4 subcarriers. The channel state is denoted at UE side by:$\tilde{H} = [\tilde{H}(1), \tilde{H}(2), \dots, \tilde{H}(N_k)]$, where $\tilde{H}$ is the channel matrix in frequency domain, $\tilde{H}(k)$ is the channel state from k-th frequency domain feedback granularity.

A further overhead reduction is achieved by DFT-based transformation

mechanism, as shown in [27], where $\widetilde{H}$ is transformed into the antenna-delay domain or angular-delay domain through a DFT (discrete fourier transform) operation. In this work, $\widetilde{H}$ is transformed into the antenna-delay domain denoted as $H = F_d\widetilde{H}$, and truncate the transformed channel state information according to the large delays, i.e.,$H = [H(1), H(2), \dots, (N_d)]$, where H is the channel matrix in time domain and N_d is the number of time domain feedback granularity, $N_d < N_k$.

In the end, the total number of feedback coefficients turns out to be $N = N_d \times N_t \times N_r$. Following the CsiNet mechanism, a UE encodes H to a M-dimensional vector S through a CsiNet –encoder and forwards the coefficients to the BS, and the BS decodes the received vector S to H' through a CsiNet-decoder to recover the full channel information on the BS side. After that, BS can utilize H' to evaluate matched codebook and schedule UE accordingly. In addition, $N_t = 32$, $N_r = 4$, $N_k = 156$, $N_d = 32$, and NMSE (normalized mean squared error) is used as the criterion to evaluate the difference between the recovered channel H' and the original channel H, which is quantified by $\mathrm{NMSE} = \mathrm{E}\left\{\left\|H' - H\right\|_2^2 / \|H\|_2^2\right\}$

As for channel models, Clustered Delay Line (CDL) channel models, which are proposed by 3GPP for link-level simulations. CDL models are defined for the full frequency range from 0.5 GHz to 100 GHz with a maximum bandwidth of 2 GHz. Three CDL models, namely CDL-A, CDL-B and CDL-C are constructed to represent three different channel profiles for NLOS while CDL-D and CDL-E are constructed for LOS [25]. The key parameters of a CDL channel are angle-of departure, angle-of arrival, cluster delay, etc., which reflect the spatial-frequency channel condition for various scenarios. Here, Table 4.3 gives a typical setting for CDL-A. Each CDL model can be scaled in delay so that the model achieves a desired RMS (Root Mean Square) delay spread, and also can be scaled in angles so that the model achieves desired angle spreads. Typical settings for the Delay Spread scaling are shown in Table 4.4, which range from 10ns to 1000ns. More detailed descriptions can be found in 3GPP Specification 38.901 [25].

Two CSI feedback methods are briefly presented then, i.e. Type1 and Type2

codebook based CSI feedback schemes, which have been standardized and widely adopted in the current 5G system to support advanced MIMO transmission. These two types are both consisting of 2D DFT based beams, and they enable the beam selection and co-phase combining between two polarizations. W_2 represents the beam selection and co-phasing between two polarizations. For Type II codebook, it is designed to have a more precisely quantification capability than type I codebook since a more accurate CSI feedback is needed. The precoding matrix is given by $W = W_1 \widetilde{W}_2 W_f^H$, where W_1 has the same definition as Type1 codebook, $\widetilde{W}_2$ is the lineal combination coefficient matrix, and $W_f = [f_0 \dots f_{M-1}]$ is the frequency domain compressed DFT matrix while $M = \lceil p \times N_{sb} \rceil$ is the number of DFT basis vectors, p is a preconfigured factor and N_{sb} is the number of subbands.

Table 4.3 Typical setting for CDL-A

Cluster #	Normalized delay	Power in [dB]	AOD in [°]	AOA in [°]	ZOD in [°]	ZOA in [°]
1	0.0000	-13.4	-178.1	51.3	50.2	125.4
2	0.3819	0	-4.2	-152.7	93.2	91.3
3	0.4025	-2.2	-4.2	-152.7	93.2	91.3
4	0.5868	-4	-4.2	-152.7	93.2	91.3
5	0.4610	-6	90.2	76.6	122	94
6	0.5375	-8.2	90.2	76.6	122	94
7	0.6708	-9.9	90.2	76.6	122	94
8	0.5750	-10.5	121.5	-1.8	150.2	47.1
9	0.7618	-7.5	-81.7	-41.9	55.2	56
10	1.5375	-15.9	158.4	94.2	26.4	30.1
…						

Table 4.4 Typical settings for the delay spread scaling

Model	Desired Delay Spread
Very short delay spread	10 ns
Short delay spread	30 ns
Nominal delay spread	100 ns
Long delay spread	300 ns
Very long delay spread	1000 ns

The concept of CsiNet is firstly introduced in [27], where the channel matrix is treated as an image, such that the AI based compressing/recovering mechanism can be straightforwardly applied. As a quintessential example in [27], a channel with 32 delays, 32 transmitting antennas and 1 receiving antenna can be treated as an image with 32*32 pixels, in which each pixel corresponds to a channel quality under specific conditions(including real and imaginary parts), e.g. one delay profile being experienced from one transmitting antenna. Regarding the processing algorithm of the basic CsiNet, a encoder first extracts channel feature by convolution operation in a convolutional layer (conv-layer). Then, a fully connected (FC) layer with 512 neurons is adopted to compress the CSI features to a lower dimension. At the decoder side, a dual operation is envisioned, where the received CSI features will go through an up-dimensioning de-compressor with FC layer and the output vector is reshaped with the same size of the original channel matrix. In the end, the reshaped vector is further fed into several RefineNet blocks to continuously refine the channel reconstruction.

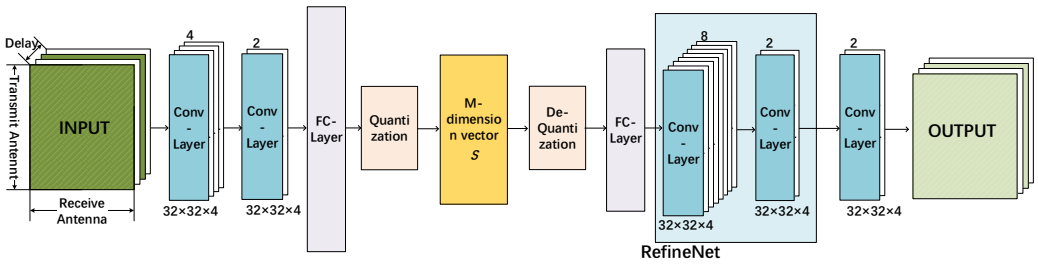

Fig. 4.5 Architecture of CsiNet-Model

Inspired by the previous works, a modified CsiNet-Mode1 is proposed and apply it to a more realistic channel model based on the assumption in 3GPP. The infrastructure of CsiNet-Mode1 is shown in Fig. 4.5. It is seen that, compared with the basic CsiNet, three main modifications are proposed.

Firstly, a different MIMO system is considered with 32 transmitting antennas and 4 receiving antennas. Moreover, the dimension of convolution kernels as well as the size of conv-layers and FC-layers in the basic CsiNet is re-adjusted to match the channel structure. Specifically, this requires the following two adjustments: (1) the input/output of CsiNet-Mode1 is adjusted to a 3-dimention block with 32×32×4

pixels, corresponding to the characteristics of delay, transmitting antenna and receiving antenna of the channel matrix respectively; (2) because of the input/output expansion of CsiNet-Mode1, the input of the first FC-layer and the output of the last FC-layer are expanded as well, and 3-dimention kernels with size 3×3×3 are applied to each conv-layer accordingly considering the correlation among adjacent transmitting antennas, receiving antennas and time domain feedbacks. Secondly, an extra conv-layer with 4 feature maps is added in the encoder to further extract channel information. With this change, 3dB gain in terms of NMSE can be observed through simulations compared to that using the basic CsiNet model. Thirdly, since higher number of the convolution layers will obviously increase the computational complexity. Only one RefineNet unit is used in the decoder and remove the second conv-layer with 16 feature maps in the unit, which from the simulation leads to a tremendous reduction of the computational complexity for this new model.

Simulations are provided to evaluate the performance of the proposed CsiNet-Mode1. Type1 and Type2 codebook based CSI feedback schemes are used as a comparison. Besides, an ideal CSI feedback scheme is considered as a reference to provide an upper bound on the performance of any CSI feedback scheme algorithm. It assumes the perfect knowledge of channel information at the BS side.

Table 4.5 Key parameters for the simulation

Parameter	Value
Carrier Frequency	3.5GHz
Bandwidth	10MHz
Subcarrier spacing	15KHz
RB number	52
N_t	32
N_r	4
N_k	156
N_d	32
N	4096 complex coefficients
Rank adaptation	On
AMC	On
Channel Model	CDL-A300
Ideal Channel estimation	Ideal

Type I Channel estimation	MMSE
N_{sb} (for type1 and type2)	10
L (for type2)	6
p (for type2)	0.25
$N_{r,u}$ (for MU-MIMO)	2
u (for MU-MIMO)	2

In order to consider more realistic situations, the clustered-delay-line model (CDL-A with RMS of delay spread 300ns) is utilized to generate multiple-path MIMO fading channels according to 3GPP channel assumptions [25]. Some key parameters for the simulation are listed in Table. 4.5. To be noted, rank adaption allows transmit different number of streams in accordance with different propagation environments, and the maximum number of ranks supported in simulation is 2. Adaptive Modulation and Coding refers to the matching of modulation and coding scheme under the radio link condition. The subband is the minimum granularity for type1 and type2 precoding, different subband allows feedback different precoding matrix.

Besides, to generate the training and testing samples for the CsiNet-Mode1, two sets of channel matrices are built through CDL-A300 channel model accordingly. It is realized by generating 20000 channel realizations from 20000 UEs for a training set and another 20000 time-varying channel realizations from a given UE for a test set.

The spectral efficiency (SPE) is used in simulations as the performance measure and it is computed by averaging over 10000 simulations.

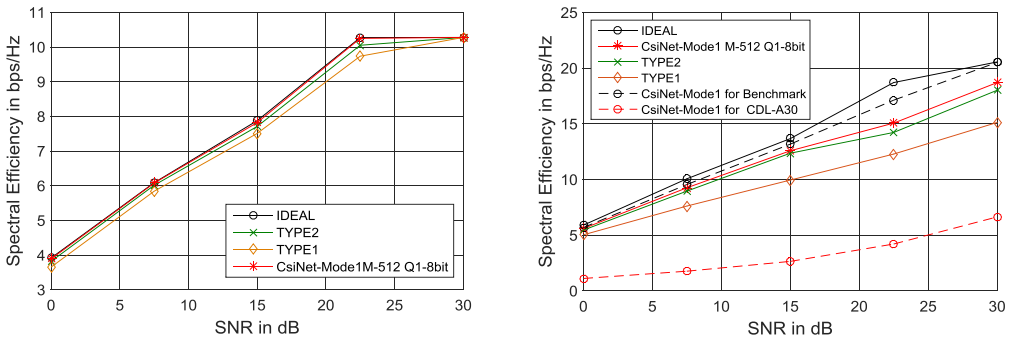

Fig. 4.6 Spectral efficiency with respect to CsiNet-Mode1, NR TYPE1 and TPYE2 CSI feedback performance. (a) Simulation on SU-MIMO, (b) Simulation on MU-MIMO.

Firstly, SPE performance is evaluated in a SU-MIMO system. The result in Fig. 4.6(a) shows that the spectral efficiency of the system based on CsiNet-Mode1 with a

512-length feedback vector almost aligns with the performance of ideal CSI feedback assumption. Obviously it is better than that of NR TYPE1 and TYPE2 mechanisms. That means, in the above simulation, the method based on AI could feedback sufficient channel characteristics, so as to achieve the same SPE as the ideal channel feedback.

At this stage, this comparable performance is indeed an encouraging result, since TYPE1/2 based CSI feedback methods have been studied for a long time, while the AI based approach is just on the horizon, more potential enhancements can be exploited.

Further, simulations in a MU-MIMO system are carried out with $u = 2$ users, the base station has $N_t = 32$ transmit antennas, and each UE has $N_{r,u} = 2$ receive antennas. The total number of receive antennas of all UE can be expressed as $N_r = \sum_{u=1}^{u} N_{r,u}$, i.e., $N_r = 4$. The location of two paired UE are conjugated, chosen for good MU performance. The azimuth angle of arrival (AOA), zenith angle of arrival (ZOA), and zenith angle of departure (ZOD) of the both UEs are set to 0, 90, 90 degree respectively. The azimuth angle of departure (AOD) of one UE is set to 18 degree while another UE is set to -18 degree.

The experimental results reveal that the SPE performance based on CsiNet-Mode1 and TYPE2 approaches are similar to each other, and they are still better than that of TYPE1 based method. Meanwhile, a benchmark for the MU-MIMO simulation is set as a comparison. The CsiNet-Mode1 used for the benchmark is trained by a UE with 20000 time-varying channels and tested with the same UE through another 20000 time-varying channels. We illustrate it here to show that if a model is accommodated with a specific channel it could lead to an excellent CSI feedback and SPE performance. On the other hand, if it is not accommodated with the channel in some cases, the performance would decline sharply. A similar conclusion is obtained in the case of CDL-A30 as shown in Fig. 4.6(b), where the CDL-A300 training model is applied to a UE with CDL-A30 channel, and the hypothesis of delay spread is completely different.

4.2.3 Detection and link adaption

For the current mobile system, basic implementation process of adaptive modulation and coding is using the feedback of channel conditions, namely CQI, PMI, RI, to control data coding and modulation through a fixed mapping algorithm. When the channel conditions are good, system can select a higher code rate to get better performance. However, the problem with this approach is that the algorithm is relatively fixed and cannot match the requirements very accurately, and can only improve the average performance. At the same time, the granularity of coding and modulation adjustment is relatively large, otherwise it will cause large signaling overhead.

In the future, as the RAN architecture gradually evolves toward cloudification, and at the same time, computing power will be everywhere, AI algorithms can be more conveniently deployed on the RAN side. For adaptive modulation and coding, the following architecture shown in Fig. 4.7 can be used, that is, through relevant parameters, features are extracted, and samples are used to train the network to obtain the mapping relationship between input and output. Through neural network generalization, relatively few training samples can be used to obtain the prediction results of the overall state space, and the modulation mode can be adjusted in real-time but doesn't cause overhead, performance will be from the original average optimal to real-time optimal.

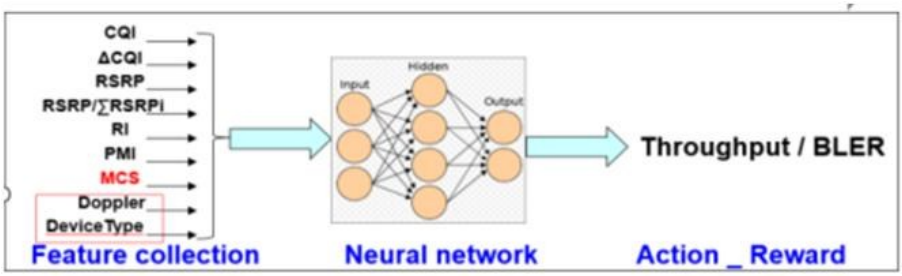

Fig. 4.7 The illustration of adaptive modulation and coding detection via AI techniques

In addition, AI techniques can also be applied in DMRS detection, i.e., the estimation of various channels. In order to achieve a satisfying detection performance, DMRS takes up a considerable part of the resource overhead. At present, the common algorithm is to use the frequency-domain correlation and time-domain correlation of

the resources occupied by DMRS to perform various linear filtering such as Wiener filter, and then to differentiate the channel information of the full-frequency position and time-domain position. The relevant information of multiple dimensions, such as frequency domain, time domain and airspace, can be effectively utilized to further improve the performance of signal detection and reduce the overhead of all kinds of reference signals.

The application of AI in DMRS detection can improve the performance of DMRS detection and reduce the cost of DMRS. Consider a downlink communication system in which the base station is equipped with a single transmitting antenna and the user is equipped with a single receiving antenna. In the frequency domain, there are a total of 20 Resource blocks (RB), and each RB has 12 subcarriers. In the time domain, the base station is sent according to the time slot, and each slot has 14 symbols. DMRS occupies 6 subcarriers per RB and 1 symbol per slot. The TDL-C channel model in the 3GPP protocol was adopted, with a time delay of 300 ns, a carrier frequency of 3.5g Hz, a SNR of 10dB, and a moving speed of 3kmph. The number of training sets and verification sets is 120,000 and 40,000 respectively. The loss function is the Mean Square Error (MSE) between the final network output and the true value. The training method is Adam algorithm commonly used in neural network.

The results are presented in the following Table 4.6 and Table 4.7. Compared with traditional communication algorithms, MSE can be further reduced. After experimenting with different network structures, we found that a simple two-layer hidden layer was good enough. Besides, the performance can be further improved when considering correlations in time domain.

TABLE 4.6 Performance comparison between AI enabled DMRS detection and conventional counterparts.

Algorithm description	NMSE
Setting 1: Two fully-connected hidden layers with neurons 960 and 3840, respectively	5.16e-3
Setting 2: Two fully-connected hidden layers with neurons 2400 and 12000, respectively	4.85e-3
Conventional algorithm based on Wiener filter MMSE detection	7.9e-3

TABLE 4.7 Performance comparison between AI enabled DMRS detection and conventional counterparts with time-correlation.

Algorithm description	NMSE
Setting 1 with conventional DMRS overhead	4.85e-3
Setting 1 with 25% DMRS overhead	5.69e-3
Conventional algorithm based on Wiener filter MMSE detection	7.9e-3

4.2.4 NOMA design framework

Non-orthogonal multiple access (NOMA) will provide massive connectivity for future Internet of Things. However, the intrinsic non-orthogonality in NOMA makes it non-trivial to approach the performance limit with only conventional communication-theoretic tools. In this work, we resort to deep multi-task learning for end-to-end optimization of NOMA, by regarding the overlapped transmissions as multiple distinctive but correlated learning tasks.

A multi-task DNN framework of NOMA (namely DeepNOMA) is proposed by treating non-orthogonal transmissions as multiple distinctive but correlated tasks. DeepNOMA uses an auto-encoding structure, which consists of a channel module, a signature mapping module (namely DeepMAS), and a detection module (namely DeepMUD) [34].

Data-driven end-to-end optimization on the transceivers is enabled by minimizing the overall cross-entropy reconstruction loss. A multi-task balancing technique is also developed to guarantee fairness among users and to avoid local optima, where objective function is derived by weighted summing over the optimization targets of the N tasks.

DeepMAS: Note that uplink NOMA users adopt a distributed fashion to map source messages to the transmit signals. Hence, we deploy N disconnected MAS mapping DNNs in DeepMAS as shown in Fig. 4.8. Any form of feed-forward DNNs can be considered, such as fully-connected DNN (FC-DNN) and convolutional NN (CNN). To make the proposed framework generalize to both sparse and dense NOMA schemes, an RE mapping layer is introduced to bring sparsity, if needed. If DeepMAS is parameterized by FC-DNN, the trained MAS mappings may not have irregular

shapes, i.e., the transmit signal alphabet on each RE does not have regular geometric shapes, unlike the conventional QAM constellations. However, for ease of hardware implementation, transmit signal alphabets are required to be constrained to certain shapes. Hence, we introduce shape prior into the network structure of DeepMAS. As an example, we consider a case where the complex symbol on each dimension of MAS has the shape of parallelogram. The N parallel outputs of DeepMAS are then superimposed in the channel module.

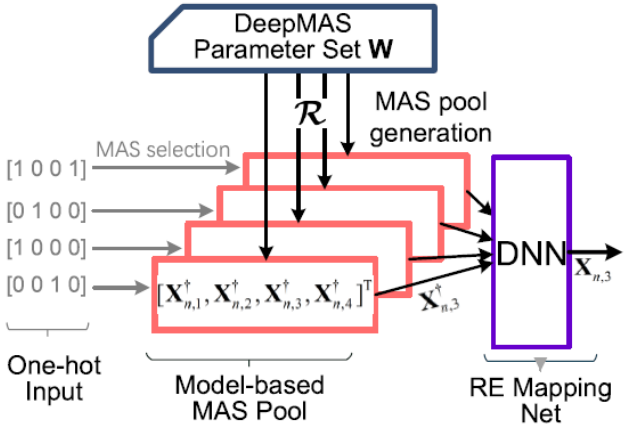

Fig. 4.8 Model-based network structure for DeepMAS

DeepMUD: DeepMUD mainly focuses on the message recovery tasks given received signal. To cope with N transmission tasks, DeepMUD consists of a public part and N task-specific private parts, as shown in Fig. 4.9. The public part firstly converts the highly-condensed received signal to a high-dimensional feature vector shared by all tasks, for the ease of signal decomposition. With the converted feature vector, the private part is able to deploy a relatively simple structure to extract the private feature vector of each task for message recovery. Without the public part, each private part shall respectively conduct the feature conversion without the knowledge provided by other tasks. This certainly increases the network complexity and makes the learning much harder.

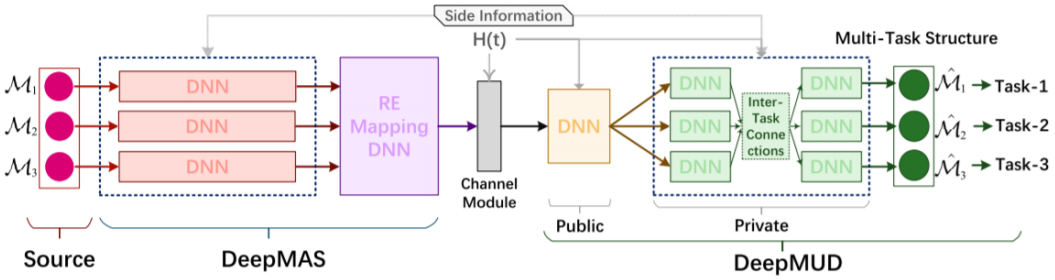

Fig. 4.9 General architecture of the proposed DeepNOMA framework using multi-task DNN.

The major obstacle lays in the very complicated signal space of received signal caused by different fading states of users. To tackle the challenge of NOMA detection in fading channels, we propose a sophisticated design of DeepMUD, where the superposition signal structure of received signal is exploited by introducing Interference Cancellation (IC)-enabled DNN units as inter-task interactions (namely ICNN). Fig. 4.10 presents the conceptional structures of FC-DNN, multi-task DNN and ICNN. By incorporating ICNN as the interplays among multiple tasks in DeepMUD, the highly condensed input signal can be decomposed into several less-interfered signal streams, which promotes the learning efficiency.

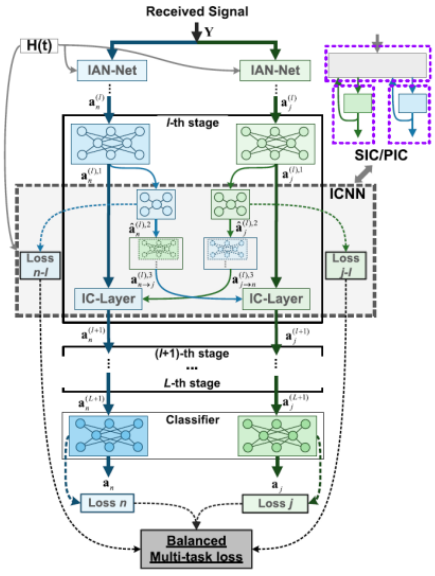

Fig. 4.10 The detailed architecture of ICNN-based DeepMUD

Some design examples of DeepMAS are provided in Fig. 4.11 and Fig. 4.12. To generate linear DeepMAS, we assume QPSK modulation and parameterize the linear spreading signatures with learnable parameters. After end-to-end training, a learned

signature set is shown in Fig. 4.11. To generate non-linear DeepMAS, we set the constellation prior as parallelogram and conduct end-to-end training. Fig. 4.12 depicts the multi-dimensional constellations on 4 REs learned by the 6 users, where different shapes represent different users. For illustration, we focus on the user represented by the green squares, and use the arrows to reflect the transmit powers of the complex symbols on different REs. In this case, the user has the minimum transmit power on RE-1, but has the maximum transmit power on RE-2 compared with the other users. Other users also hold diversified transmit powers on different REs, which naturally leads to the power gain differences among users. This fact promotes the efficiency of interference cancellation among users and thus enhances the detection accuracy.

$$S_{4\times 6} = \begin{bmatrix} 0.53+0.035i & -0.39-0.32i & 0.16-0.25i & -0.11-0.46i & -0.25+0.38i & 0.50-0.43i \\ 0.0043-0.10i & -0.33+0.40i & 0.32+0.42i & 0.22-0.24i & -0.76+0.0040i & -0.51-0.060i \\ 0.35-0.23i & -0.0980+0.32i & 0.54-0.36i & 0.75+0.25i & 0.37-0.16i & 0.070-0.057i \\ 0.62+0.37i & -0.33+0.50i & -0.44-0.10i & -0.15-0.16i & 0.07-0.23i & 0.0026+0.56i \end{bmatrix}$$

Fig. 4.11 A design example of linear DeepMAS

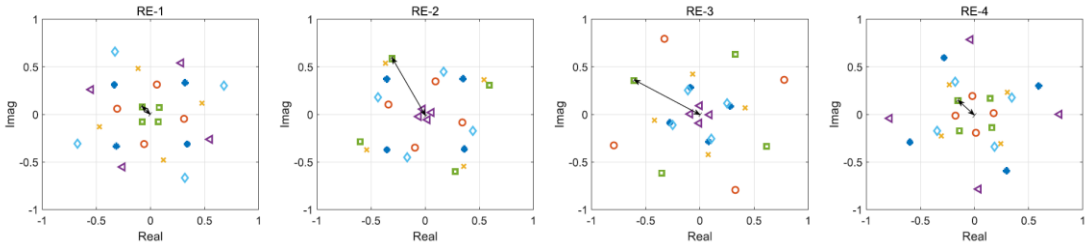

Fig. 4.12 A design example of non-linear DeepMAS, with different shapes representing different users.

In Fig. 4.13, link-level simulations are performed to evaluate the performance of DeepNOMA in various channel models. Detailed experiments and link-level simulations show that higher transmission accuracy and lower computational complexity can be simultaneously achieved by DeepNOMA under various channel models, compared with state-of-the-art.

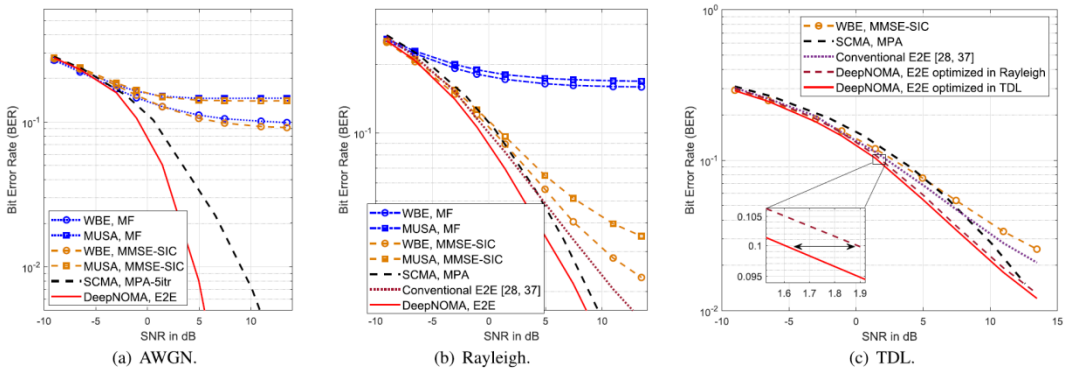

Fig. 4.13 Performance of DeepMUD in fading channel models. Overloading factor N/K = 150%.

4.2.5 End-to-end learning

The physical layer standardization design has always been closely related to the implementations of physical layer transceivers, which has taken the form of a sequential module-by-module realization since the initial commercialized communications, e.g., coding, modulation, waveform, and multiple antennas. Such realization incurs heavy and complicated internal interfaces and control signaling. The emerging AI-enabled physical layer approaches could fundamentally break through the limitations of conventional module-by-module transceiver realizations. As proposed in [35], the physical layer transceivers could be implemented through advanced ANNs.

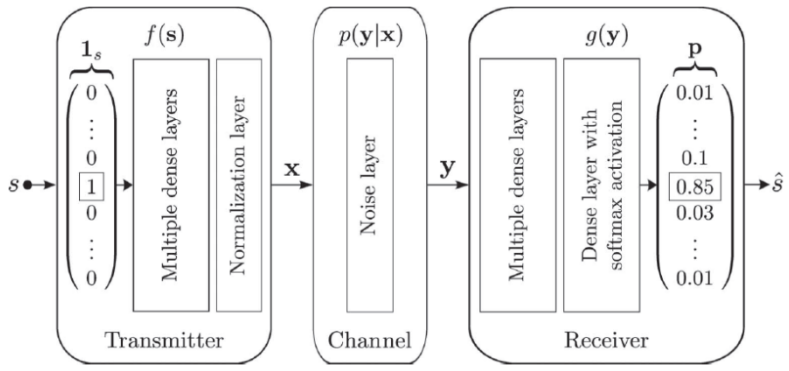

Fig. 4.14 Implementation of autoencoder based end-to-end learning for wireless communication [35]

Specifically, as illustrated in Fig. 4.14, the whole wireless link including transmitter, wireless channel, and receiver is implemented via an autoencoder neural network. The autoencoder is a classical network structure in representation learning, where the input and the output of the network are configured to be the same signal, and the network is trained to learn a (sparse) representation of input given by the internal feature of the network. However, in communications, the autoencoder is utilized to mimic the structure of transmitter and receiver, and the internal feature is treated as the sent (received) signal. In fact, such autoencoder learns how to adjust the input signal to combat the signal distortion brought by wireless channels. Since the learning procedure of autoencoder includes the optimization of both transceivers, it is usually termed as end-to-end learning. The very seminal idea of end-to-end learning is proposed in [35], where the authors compare the learned results to simple coding and modulation designs (such as (7, 4) Hamming coding and BPSK) to demonstrate the feasibility of such ideas. The initial design of end-to-end learning is too simple to be implemented in practical systems as only a trivial AWGN channel is considered, and issues such as successive transmission are still open problems.

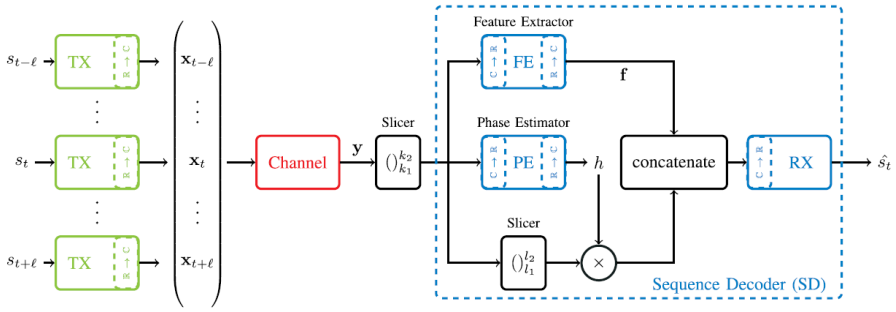

Fig. 4.15 Implementation of autoencoder based end-to-end learning for successive transmission

Soon after the seminal work in [35], the authors in [36] investigated how to realize successive transmission in a system solely consisting of neural networks. The same end-to-end learning principle as in [35] is utilized, but the network structure changes. The most distinguishing difference is that the newly developed network in Fig. 4.15 accepts a sequence of signals as input, and utilizes slicers to restore each

message. A feature extractor and a phase extractor are adopted to accomplish the synchronization procedure. The synchronized signal as well as the extracted feature is then fed to the receiver, which is implemented via conventional network structure. By considering multiple successive messages in one training epoch, the auto-encoder could learn a joint modulation and coding scheme between multiple symbols. While the implementation in Fig. 4.15 is novel in principle, it is quite complicated, especially compared with the synchronization mechanism designed by expert knowledge. A natural concern arises that is it suitable or convenient for the neural networks to realize all communication modules? In fact, there are solutions for neural networks to handle synchronization issues (though complicated), while, however, it is extremely challenging for a system solely consisting of neural networks to address other issues such as multi-path fading.

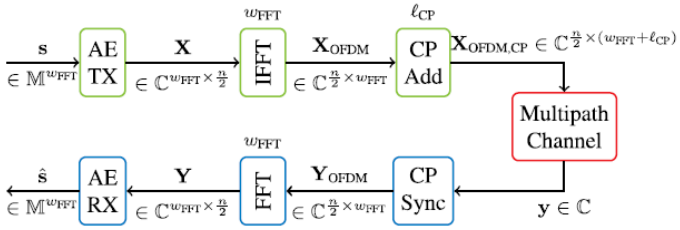

Fig. 4.16 OFDM based implementation of end-to-end learning

Towards the question aforementioned, the authors in [37] proposed a hybrid end-to-end learning system with OFDM implementation. The idea is illustrated in Fig. 4.16, where the output of transmitter (implemented via neural networks) is processed by an IFFT and a CP adding module. In other words, the multi-path fading and synchronization issue are addressed through OFDM techniques and the autoencoder is left to handle the joint optimization of modulation and coding. An interesting module is the channel estimation, which could be either implemented via neural networks or conventional methods. If channel estimation is implemented via neural networks, a superimposed pilot and data design can be learned with a comparable performance to classical minimum mean square error (MMSE) method.

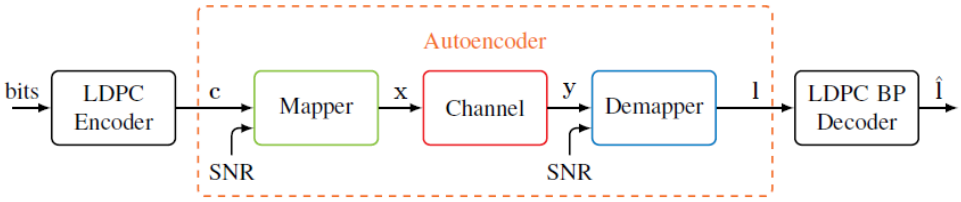

Fig. 4.17 Bit-wise autoencoder setup with an LDPC outer code [38]

Apart from the hybrid design in OFDM systems, end-to-end learning can also be integrated with existing channel codes as shown in Fig. 4.17. The authors in [38] proposed to learn a joint optimization of constellation shaping and labeling with an existing LDPC code serving as a general outer code. In addition, a bit-wise mutual information based loss function is also adopted to make the proposed scheme closer to actual systems. The proposed system is also implemented on software-defined radios (SDRs) and trained based on the actual wireless channels to verify the viability. Experimental results reveal that the proposed method enables significant gains compared to conventional techniques.

Due to the challenges in data collecting and data size, the current physical layer end-to-end learning results are trained based on simulated data generated by statistical channel models. In fact, it is very challenging for these statistical channel models to exactly characterize all channels in the real radio environments channel. Therefore, the performance of end-to-end learning cannot be guaranteed when training on simulated data, which promotes the necessity of learning on data from real radio environment. At least for now, AI enabled end-to-end learning of transceivers is still a controversial topic in air-interface design, especially for the industry. Implementing end-to-end learning in practical systems requires a significant change in the current air-interface framework, which seems quite unrealistic now. However, it cannot be denied that such end-to-end design could have a profound impact on the wireless communications in the long term.

5 Conclusion and development trend of air interface technology

On the one hand, spectral efficient transmission schemes are essential to enhance the air interface capability, e.g. by advanced coding & modulation. On the other hand, we also need more spectrum to fulfill the extreme user experience. Detailed comments referring to specific technologies can be found as follows:

(1) Code and modulation schemes which can approach the Shannon's capacity bound are still required.

(2) Conventional OFDM waveform shows some inadequacies for some 6G scenarios, e.g. high speed, high frequency and etc. Enhanced waveforms based on OFDM is required facing diversified 6G scenarios.

(3) The multiple access will be expanded from human-centric, grant-based scheme to autonomous-things centric, grant-free scheme.

(4) For practical usage, MIMO will be enhanced by new antenna structures, new deployment, new signal processing, novel applications and etc.

(5) In the future, the combination of multi-dimensional heterogeneous networking and 6G cellular network will further improve network coverage and user experience rate.

(6) In terms of channel estimation and CSI feedback, signal detection and link adaptation, wireless AI shows certain advantages compared with traditional schemes.

(7) AI can play a certain role in the end-to-end framework optimization, but the related research is still in the early stage, and the specific scenarios and use cases need to be further explored.

(8) Data acquisition and privacy protection in wireless AI are also the focus of attention.

(9) The integration of HI and AI is one of the main development directions of wireless AI.

Reference

[1] Liu G, Huang Y, Li N, et al. Vision, Requirements and Network Architecture of 6G Mobile Network beyond 2030[J]. 中国通信, 2020(9).

[2] 易芝玲, 王森, 韩双锋, et al. 从 5G 到 6G 的思考:需求,挑战与技术发展趋势[J]. 北京邮电大学学报, 2020(2): 1-9.

[3] L. Zhang, Y. Liang, D. Niyato, "6G Visions: Mobile ultra-broadband, super internet-of-things, and artificial intelligence", China Communications, Vol. 16, Issue 8, 2019.

[4] Z. Zhang, Y. Xiao, Z. Ma et al., "6G Wireless Networks: Vision, Requirements, Architecture, and Key Technologies," IEEE Vehicular Technology Magazine, vol. 14, no. 3, 2019, pp. 28-41.

[5] B. Zong, C. Fan, X. Wang et al., "6G Technologies: Key Drivers, Core Requirements, System Architectures, and Enabling Technologies", IEEE Vehicular Technology Magazine, Vol. 14, Issue 3, 2019.

[6] K. B. Letaief, W. Chen, Y. Shi et al., "The Roadmap to 6G: AI Empowered Wireless Networks", IEEE Communications Magazine,vol. 57, issue 8, 2019.

[7] Cover T M, Thomas J. A. Elements of Information Theory[M]. Hoboken-New Jersey: Wiley & Sons, Inc., 2006: 303-307.

[8] 中国移动研究院. 2030+愿景与需求报告（V1）[EB/OL].广州-中国: 中国移动, 2019(2019-11-15)[2020-4-7].http://cmri.chinamobile.com/wp-content/uploads/2019/11/2030 愿景与需求报告.pdf

[9] Chen Shanzhi, Liang Yingchang, Sun Shaohui, et al. Vision, requirements, and technology trend of 6G: how to tackle the challenges of system coverage, capacity, user data-rate and movement speed[J]. IEEE Wireless Communications, 2020, 27(2): 218-228.

[10] Chih-Lin I, Han S , Xu Z , et al. New Paradigm of 5G Wireless Internet[J]. IEEE Journal on Selected Areas in Communications, 2016, 34(3):1-1.

[11] J. Liu, W. Liu, X. Hou, Y. Kishiyama, L. Chen and T. Asai, "Non-Orthogonal Waveform (NOW) for 5G Evolution and 6G," 2020 IEEE 31st Annual International Symposium on Personal, Indoor and Mobile Radio Communications (PIMRC), London, United Kingdom, 2020, pp. 1-6

[12] S. Sugiura, “Frequency-domain Equalization of Faster-than-Nyquist Signaling,” IEEE Wireless Communications Letters, vol. 2, no. 5, pp. 555–558, 2013.

[13] HUM S V, PERRUISSEAU-CARRIER J. Reconfigurable large surfaces are needed to beat relaying[J]. IEEE Wireless Communications Letters, 2020,9(2): 244248.

[14] HUANG C, HU S, ALEXANDR OPOULOS G C, et al. Holographic MIMO surfaces for 6G wireless networks: opportunities, challenges, and trends [EB/OL]. (2020-0419) [2020-04-25]. https://arxiv.org/abs/1911.12296.

[15] University of Oulu. Key drivers and research challenges for 6G ubiquitous wireless intelligence[EB/OL]. (2019-09-01) [2020-04-25]. http://jultika.oulu.fi/files/isbn9789526223544.pdf.

[16] Tomas J P. NTT DoCoMo, Metawave test 5G mobile system in Tokyo [EB/OL]. (2018-12-06)[2020-04-25]. http://www.srrc.org.cn/en/news4504.aspx.

[17] ARUN V, BALAKRISHNAN H. RFocus: practical beamforming for small devices[EB/OL]. (2019-0513)[2020-04-25]. https://arxiv.org/abs/1905.05130.

[18] DAI L, WANG B, WANG M, et al. Reconfigurable intelligent surface-based wireless communications: antenna design, prototyping, and experimental results[J]. IEEE Access, 2020(8): 45913-45923.

[19] TANG W, DAI J Y, CHEN M, et al. Programmable metasurface-based RF chain-free 8PSK wireless transmitter[J]. Electronics Letters, 2019,55(7): 417-420.

[20] TAHA A, ALRABEIAH M, ALKHATEEB A. Enabling large intelligent surfaces with compressive sensing and deep learning[EB/OL]. (2019-04-23)[2020-04-25]. https://arxiv.org/abs/1904.10136.

[21] W. Liu, X. Hou, Y. Kishiyama, L. Chen and T. Asai, "Transform Domain Precoding (TDP) for 5G Evolution and 6G," in IEEE Signal Processing Letters,

vol. 27, pp. 1145-1149, 2020.

[22] 3GPP, "3GPP TS 38.212 V16.1.0 3rd Generation Partnership Project; Technical Specification Group Radio Access Network; NR; Multiplexing and channel coding (Release 16)", Tech. Rep., 2020

[23] 3GPP, "3GPP TS 38.214 V16.1.0 3rd Generation Partnership Project; Technical Specification Group Radio Access Network; NR; Physical layer procedures for data (Release 16)", Tech. Rep., 2020

[24] 3GPP, "3GPP TS 38.331 V16.0.0 3rd Generation Partnership Project; Technical Specification Group Radio Access Network; NR; Radio Resource Control (RRC) protocol specification (Release 16)", Tech. Rep., 2020

[25] 3GPP, "3GPP TR 38.901 V16.1.0 3rd Generation Partnership Project; Technical Specification Group Radio Access Network; Study on channel model for frequencies from 0.5 to 100 GHz (Release 16) ", Tech. Rep., 2020

[26] T. Wang et al., "Deep learning for wireless physical layer: Opportunities and challenges," *China Commun.*, vol. 14, no. 11, pp. 92–111, Nov. 2017.

[27] C.-K. Wen, W.-T. Shih, and S. Jin, "Deep learning for massive MIMO CSI feedback," *IEEE Wireless Commun. Lett.*, vol. 7, no. 5, pp. 748–751, Oct. 2018.

[28] C. Lu, W. Xu, H. Shen, J. Zhu, and K. Wang, "MIMO channel information feedback using deep recurrent network," *IEEE Wireless Commun. Lett.*, vol. 23, no. 1, pp. 188–191, Jan. 2019.

[29] T. Wang, C.-K. Wen, S. Jin, and G. Y. Li, "Deep learning-based CSI feedback approach for time-varying massive MIMO channels," *IEEE Wireless Commun. Lett.*, vol. 8, no. 2, pp. 416–419, Apr. 2019.

[30] J. Guo, C.-K. Wen, S. Jin, and G. Y. Li, "Convolutional neural network-based multiple-rate compressive sensing for massive MIMO CSI feedback: Design, Ssimulation, and analysis," IEEE Trans. Wireless Commun., vol. 19, no. 4, pp. 2827–2840, Apr. 2020.

[31] X. Li, H. Wu, "Spatio-Temporal Representation with Deep Neural Recurrent Network in MIMO CSI Feedback," *IEEE Wireless Commun. Lett.*, vol. 9, no. 5, pp. 653–657, Jan. 2020.

[32] T. Chen, J. Guo, S. Jin, C.-K. Wen, and G. Y. Li, "A novel quantization method for deep learning-based massive MIMO CSI feedback," in *Proc. GlobalSIP*, Ottawa, Canada, 2019.

[33] C. Lu, W. Xu, S. Jin, and K. Wang, "Bit-level optimized neural network for multi-antenna channel quantization," Sep. 2019, arXiv:1909.10730. Available: https://arxiv.org/abs/1909.10730

[34] N. Ye, X. Li, H. Yu, L. Zhao, W. Liu and X. Hou, "DeepNOMA: A Unified Framework for NOMA Using Deep Multi-Task Learning," *IEEE Trans. Wireless Commun.*, vol. 19, no. 4, pp. 2208-2225, Apr. 2020.

[35] T. O'Shea and J. Hoydis, "An introduction to deep learning for the physical layer," *IEEE Trans. Cog. Commun. Netw.*, vol. 3, no. 4, pp. 563–575, 2017.

[36] S. Dörner, S. Cammerer, J. Hoydis, and S. T. Brink, "Deep learning based communication over the air," *IEEE J. Sel. Topics Signal Process.*, vol. 12, no. 1,

pp. 132–143, Feb. 2018.

[37] A. Felix, S. Cammerer, S. Dörner, J. Hoydis, and S. ten Brink, "OFDM autoencoder for end-to-end learning of communications systems," in *IEEE 19th International Workshop on Signal Processing Advancesvin Wireless Communications (SPAWC)*, 2018, pp. 1–5.

[38] S. Cammerer, F. A. Aoudia, S. Dörner, M. Stark, J. Hoydis, and S. T. Brink, "Trainable communication systems: Concepts and prototype," *IEEE Trans. Commun.*, early access, Jun. 2020.

Acknowledgments

Grateful thanks to the following contributions for their wonderful work on this whitepaper:

Contributors：

China Mobile: Sen WANG, Tian XIE, Zhen FENG

UESTC: Yue XIAO, Ping YANG

ZTE: Jin XU, Yu XIN, Yijian CHEN, Mengnan JIAN, Lei LIU

UNISOC: Runquan MIAO, Mimi CHEN

DOCOMO Beijing Labs: Wenjia LIU, Juan LIU, Xiaolin HOU

China Unicom: Hanwen CHANG, Rong HUANG

Datang Mobile: Qiuping HUANG, Haichao QIN

Ericsson: Peng LIN

NUAA: ZhenZhou TANG

vivo：Dajie Jiang, Yao JIAN

OPPO: Wenqiang TIAN, Jia SHEN

Reviewers: Sen WANG, Tian XIE, Zhen FENG, Shulun ZHAO, Siying LV

未来移动通信论坛

FUTURE MOBILE COMMUNICATION FORUM